INTERNATIONAL JOURNAL OF CURRENT RESEARCH IN CHEMISTRY AND PHARMACEUTICAL SCIENCES
(p-ISSN: 2348-5213: e-ISSN: 2348-5221)
www.ijcrcps.com
(A Peer Reviewed, Referred, Indexed and Open Access Journal)
DOI: 10.22192/ijcrcps Coden: IJCROO(USA) Volume 12, Issue 9- 2025

Research Article

DOI: http://dx.doi.org/10.22192/ijcrcps.2025.12.09.001

Green synthesis of Silver Nanoparticles with *Panchavalkala* and its Antimicrobial activity

K.P.M.W.D.A.M.A. Fernando[1], J.A.M.S. Jayatilake[2]

[1]Postgraduate Institute of Science, University of Peradeniya, Peradeniya, Sri Lanka
[2]Department of Oral medicine and Periodontology, Faculty of Dental Sciences, University of Peradeniya, Peradeniya, Sri Lanka.

Abstract

Panchavalkala is a combination of water extracts of five barks of medicinal plants which is widely used for the treatment of wounds in Ayurveda medicine. Three different combinations are commonly used as *Panchavalkala* in Sri Lanka. Recently, synthesis of silver nanoparticles (Ag-NPs) using various plant extracts has gained much attention from various sectors due to their cost effectiveness, affordability, effectiveness and Eco friendliness. Therefore, the objective of this study was to synthesize silver nanoparticles using the three different alternative combinations of *Panchavalkal*a and to assess their antimicrobial effect against some common wound pathogens. Three different combinations were prepared using barks of each plant concentrating into 8:1 by boiling and named as A, B, and C. Ag -NPs were synthesized by mixing 10 ml of each filtered extract with 90 ml of 1mM aqueous silver nitrate. The color change, UV-visible absorbance and scanning electron microscopy (SEM) confirmed the synthesized of Ag-NPs. Screening of antimicrobial activity (AMA) was carried out using the agar well diffusion assay on standard isolates of *Escherichia coli, Pseudomonas aeruginosa, Staphylococcus aureus* (MSSA), methicillin-resistant *Staphylococcus aureus* (MRSA), and *Candida albicans* as well as clinical isolates of MSSA and MRSA. Sample C had significant inhibition against MSSA compared to amoxicillin ($P = 0.005$). Sample A ($P = 0.001$) and C ($P = 0.019$) showed significant antimicrobial effect against MRSA compared to vancomycin. None of the above combinations of *Panchavalkala* had inhibitory effect on other tested organisms. However, all three *Panchavalkala* samples showed antimicrobial effect against clinical isolates of MSSA and MRSA. Except the plant *A. indicum*, other constituent plants of *Panchavalkala* had antimicrobial effect only against MSSA and MRSA. Ag-NPs synthesized from each combination of *Panchavalkala* showed antimicrobial effect against all the tested microorganisms. Ag-NPs synthesized from sample B and C showed significantly higher effects against standard of MRSA, *C. albicans* and clinical isolates of MRSA ($P= 0.000$). Sample B showed significantly higher effects against standard and clinical isolates of MSSA ($P=0.000$). In conclusion, *Panchavalkala* all three combinations were effective against MSSA and

MRSA *in vitro* while Ag-NPs synthesized from above three combinations of *Panchavalkala* were effective against all the tested microorganisms. Further studies are recommended to explore the molecular level interactions such as drug antagonism, additivism, and synergy of *Panchavalkala* and Ag-NPs.

Keywords: *Panchavalkala*, silver nanoparticles, UV-visible absorbance and scanning electron microscopy, antimicrobial activity.

1- Introduction

1.1 Background of the study

Panchavalkala is a water extract of five barks of medicinal plants which are widely used to treat infected and non-infected wounds in Ayurveda medicine since thousands of years (Chunekar, 2006). "Pancha" means five and "Valkala" means bark and *Panchavalkala* always contains five barks of medicinal plants. According to the present Ayurveda system in India, a majority uses five barks of trees namely, vernacularly Nygrodha (*Ficus benghalensis* Linn), Udumbara (*Ficus glomerata* Roxb.), Ashwatha (*Ficus religiosa* Linn.), Parisha (*Thespesia populnea* Sol. ex-correa.) and Plaksha (*Ficus lacor* Buch-Ham.) for *Panchavalkala*. Researchers, present and past have evaluated the properties such as anthelmintic, antimicrobial, wound healing, anti-inflammatory, hemostatic, and pain reliving of these plants in combination as well as individually (Dhammananda *et al*., 2016). However, some plant species contained in the Indian *Panchavalkala* combination do not grow naturally in Sri Lanka. Therefore, controversy exists over the plants used in the Sri Lankan formula of Panchavalkala, and three different combinations are commonly used in Sri Lanka as follows. One combination which was named as "A" in this study consists of Nygrodha (*Ficus bengalensis* Linn.), Udumbara (*Ficus racemosa* Linn.), Ashwatha (*Ficus religinosa* Linn.), Plaksha (*Ficus arnottiana* (Miq.) Miq.), and Vethasa (*Garcinia quaesita* Pierre.). The second *Panchavalkala* combination named as "B" consists of Nygrodha (*Ficus bengalensis* Linn.), Udumbara (*Ficus racemosa* Linn.), Ashwatha (*Ficus religinosa* Linn.), Parisha (*Thespesia populnea* Sol. ex-correa.) and Plaksha (*Abutilon indicum* (L.) Sweet.). And the third one named "C" consists of Nygrodha (*Ficus bengalensis* Linn.), Udumbara (*Ficus racemosa* Linn.), Ashwatha (*Ficus religinosa* Linn.), Plaksha (*Chrysophyllum cainito* Linn.), and Vethasa (*Garcinia quaesita* Pierre.).

Nanotechnology is the design, characterization, production, and application of structures, devices, and systems by controlling the shape and size in nanometer scale which is conventionally defined as 1 to 100 nm (1nm = one-billionth of a meter; 10-9 m) (Paulkumar *et al*., 2014). The size range is set normally to be a minimum of 1 nm to avoid single atoms or a small group of atoms being designated as nanoparticles. Therefore, nanotechnology involves individual atoms and molecules for the purpose of observing and controlling the nanoparticles (Lusia and Duncan, 2010).

Novel applications of nanoparticles (NPs) and nanomaterials are growing rapidly on various fronts due to their completely new or enhanced properties based on their size, distribution, and morphology. It is swiftly gaining revolution in many fields such as health care, cosmetics, biomedical, food and feed, drug-gene delivery, environment, health, photochemistry, energy science, etc. (Ahmed *et al*., 2016). However, over the past few decades, the use of plants with different applications in medicine and industry has been growing as well as increasingly used in the world. In recent years, many environmentally friendly methods have been employed in the synthesis of nanoparticles (Balayssac *et al*., 2009).

The biological methods for metallic nanoparticle synthesis using bacteria, fungi, proteins, polypeptides, whole plants, plant extracts, and marine algae are simple because there is no need

of using high temperature, pressure, energy, and toxic chemicals. Hence, it is affordable, and eco-friendly. These biological methods can be easily used to generate nanoparticles with acceptable size and morphology (Ghodsieh *et al*., 2017). The metallic nanoparticles contain remarkable antibacterial properties due to their large surface area to volume ratio which is of interest for researchers considering the growing microbial resistance against metal ions and antibiotics (Khalil *et al*., 2013).

Silver is one of the most commercialized nano-materials among the all-noble metal nanoparticles such as zinc, gold, copper, platinum, and lead, with five hundred tons of silver nanoparticles production per year and is estimated to increase in the next few years (Larue et al., 2014) because of its profound role in the field of high sensitivity biomolecular detection, catalysis, light emitters, single electron transistors, biosensors, and medicine. Silver nanoparticles have strong bacteriostatic and bactericidal effects as well as antifungal, anti-inflammatory, and angiogenesis activities (El-Chaghaby and Ahamad, 2011). Silver metal nanoparticles for biomedical application have been added to wound dressing, topical cream, antiseptic sprays, and fabrics. Thus, silver functions as an antiseptic and displays a broad biocidal effect against microorganisms through the disruption of their unicellular membrane and disturbing cellular enzymatic activities (Ahmed *et al*., 2016).

1.2 Significance and Justification of the study

There are several chemical and physical methods used for the synthesis of metallic nanoparticles. These methods have usually been successful in the synthesis of large quantities of nanomaterials of different sizes and shapes within a short period. However, most of those physical and chemical methods are extremely expensive and also involve use of toxic, hazardous chemicals as stabilizers which may pose potential environmental and biological risks (Kuppusamy *et al*., 2015). Therefore, in recent years, the use of biological methods for the synthesis of metallic nanoparticles has received attention because biological methods are inexpensive, eco-friendly, and can be carried out in one step (Otari *et al*., 2012). For synthesis of nanoparticles using biological methods with the plant extracts have several advantages over other green synthesis methods such as microbe mediated synthesis. It is because plants are broadly distributed, easily available, safe to handle, and less expensive and they are non-toxic and environmentally friendly (Mittal *et al*., 2013).

The synthesis of various nanoparticles of metals such as silver, gold, copper, iron. etc, is one of the most important fields in modern nanotechnology (Allafchian et al., 2016). Among the diverse metallic nanoparticles, silver nanoparticles (Ag-NPs) can be used in a wide range of applications such as water disinfection, surgical coating, biomedical, agriculture, photochemistry, engineering, and health care. Silver nanoparticles especially show various properties such as catalytical, electrochemical, conductive, and antimicrobial activity (Allafchian *et al*., 2015). In the past, silver has been recognized to be efficient against a wide range of microorganisms (Kalishwaralal *et al*., 2010) and it is also used as an antiseptic and antimicrobial agent against both Gram-negative and Gram-positive bacteria as well as fungi with the lowest cytotoxicity (Biel *et al*., 2011). Thus, silver nanoparticles exhibit a broad spectrum of bactericidal and fungicidal activity besides silver has a lower possibility for the development of microbial resistance (Salman, 2017).

Although modern antibiotics play an extremely critical role in the management of bacterial infections, bacteria have developed resistance to antimicrobials over the past few decades (Davies and Davies, 2010). Spreading and collision of drug-resistant bacteria will be a foremost challenge on human health in the future (Rajesh and Malarkodi, 2014) and antimicrobial resistance (AMR) has currently become a serious public health issue. It has been estimated that 10 million deaths annually may occur by 2050 if the AMR continues to develop (Mendelson, 2015). It will also cause high morbidity and increase treatment costs up to 100 trillion USD in 2050 (Pooja and

Tannaz, 2017). Therefore, it is an urgent requirement to develop alternative antimicrobial agents that can combat AMR. Accordingly, it is necessary to explore alternative antibacterial drugs as well as the green synthesis of silver nanoparticles and their antimicrobial effects.

The Ayurveda medical system uses individual or combination of plant material having a varied range of biological activities that can be used to manage infections due to bacteria with AMR (Ahmad and Beg, 2001). *Panchavalkala* has been widely used for the treatment of infected wounds in Ayurveda medicine. Although three different combinations of *Panchavalkala* are used in Sri Lanka, there has been no clear scientific investigation conducted to identify the effects of *Panchavalkala* on wound pathogens. According to the available literature, different combinations of *Panchavalkala* have not been studied comparatively on the same platform. Therefore, it is worthwhile to separately study the antimicrobial effects of three different combinations of Panchavalkala used in Sri Lanka and their Ag-NPs against some common wound pathogens.

1.3 Objectives of the study

This study is mainly focused on the following general and specific objectives.

1.3.1 General objective

1. To synthesize silver nanoparticles using water extracts of three alternative combinations of *Panchavalkala* and to assess their antimicrobial effect against some common wound pathogens.

1.3.2 Specific objectives

1. To identify the antimicrobial effect of three different combinations of *Panchavalkala* against standard isolates of common wound pathogens *in vitro.*
2. To identify the antimicrobial effect of three different combinations of *Panchavalkala* against clinical isolates of *Staphylococcus aureus in vitro*.
3. To identify the antimicrobial effect of individual medicinal plants used in *Panchavalkala* against common wound pathogens in vitro.
4. To green synthesize silver nanoparticles using each three-alternative combination of *Panchavalkala*.
5. To identify the antimicrobial effect of synthesized silver nanoparticles against standard isolates of common wound pathogens *in vitro*.
6. To identify the antimicrobial effect of synthesized silver nanoparticles against clinical isolates of *Staphylococcus aureus in vitro*.

1.4 Literature review

1.4.1 Literature review of *Panchavalkala*

Some previous investigations have been carried out using *Panchavalkala* which is a combination of five barks of medicinal plant including Nygrodha (*Ficus benghalensis* Linn), Udumbara (*Ficus glomerata* Roxb.), Ashwatha (*Ficus religiosa* Linn.), Parisha (*Thespesia populnea* Sol. ex correa.) and Plaksha (*Ficus lacor* Buch-Ham.) (Chunekar, 2006). Those are easily available and often used in practice and also known as *Vrunaropana* (healer of wound) because of their wound healing property (Shastri, 2001). Many research papers are available in relation to wound healing properties of *Panchavalkala*.

Antimicrobial activity of *Panchavalkala* produced in the above combination has been evaluated for its efficacy as a skin disinfectant against *Staphylococcus aureus*, *Escherichia coli*, *Pseudomonas aeruginosa*, *Candida albicans*. The study concluded that the extract of *Panchavalkala* showed more antimicrobial activity than individual ingredients of *Panchavalkala* (Khadkutkar, 2015). A study of the antimicrobial effect of alcoholic extract of *Panchavalkala* against methicillin resistant *Staphylococcus aureus* (MRSA) has demonstrated that *Panchavalkala* could control MRSA induced wound infections (Patankar and Grampurohit, 1999).

Another study has been conducted to evaluate the antimicrobial effects and wound healing property of Ayurvedic ointment comprising of *Panchavalkala* using some microorganisms causing wound infections like *E. coli*, *Staphylococcus aureus*, and *Streptococcus pyogenes*. This study showed that the *Panchavalkala* ointment enhanced the process of wound healing (Sakhitha *et al*., 2013). The gel hand wash of *Panchavalkala* has antibacterial activity particularly against *Bacillus pumillus* and *S. aureus* at a minimum concentration of 40 mcg/ml (Kamble *et al*., 2012).

The phytochemical constituents from *Panchavalkala* have been extracted and detected by various qualitative tests. Phytochemical constituents mainly were phytosterols, tannins and glycosides and had antimicrobial activity against various Gram negatives, Gram positives and fungi (Bhardwaj and Sahu, 2007). It was observed that tannins had the best antimicrobial activity in comparison with glycosides and phytosterols (Bhardwaj and Sahu, 2007). Another study revealed that *Panchavalkala* presented with high number of tannins and polyphenols and the total phenolic content ranged from 3.5% to 10.8% w/w and the total tannin content ranged from 1.6% to 7.0% w/w (Anandjiwal *et al*., 2008). Panchavalkala had good free radical scavenging activity which can be attributed to tannins and phenolics along with other compounds (Anandjiwal *et al*., 2008). High polar solvent extracts of another *Panchavalkala* combination containing *Ficus benghalensis*, *Ficus religiosa*, *Ficus tsiela*, and *Garcinia cambogia* showed antimicrobial activity against MRSA strains with a significant antioxidant activity (Gopalakrishnan *et al*., 2017).

1.4.2 Literature review of plant materials

1.4.2.1 *Ficus benghalensis* (L).

1.4.2.1.1 Taxonomic Hierarchy

Kingdom: Plantae; Subkingdom: Viridiplantae; Infrakingdom: Streptophyta; Superdivision: Embryophyta; Division: Tracheophyta; Subdivision: Spermatophytina; Class: Magnoliopsida; Superorder: Rosanae; Order: Rosales; Family: Moraceae; Genus: Ficus; Species: *Ficus benghalensis* L.

1.4.2.1.2 Plant morphology

It is a large banyan, rooting from the spreading branches, deciduous to evergreen. Leaves are spirally arranged. Twigs, stipules, petioles, the underside of lamina; and figs white puberulous, slowly glabrescent. Twigs 3-7 mm thick, light brownish ochre. Stipules stout. Lamina 10-30 × 7-20 cm, ovate, obtuse, base cordate, rarely cuneate, firmly coriaceous; lateral veins 5-6 (-7) pairs, -10 intercostals, reticulations regular and raised on both sides; basal veins 2-4 pairs, 1/3-1/2 lamina; petiole 15-70 × 3-5 mm, stout. Figs sessile, axillary, paired, ripening orange to red; basal bracts 3-7 × 10-14 mm, umbonate at the base, obtuse; body 14-17 mm wide (15-20 × 21-25 mm, living), depressed-globose, the plane orifice closed by 3 flat or sub umbonate apical bracts in a disc 3-4 mm wide; internal bristles none. Tepals 2-3 in male flowers, 3-4 in gall-and female flowers, free. Male flowers with pedicels 0.5-2.8 mm long, anther is shortly mucronate. Gall-flowers with pedicels 1.5-2.3 mm long. Female flowers are sessile. Lamina with cystoliths abundant on the upper side, few or none below; stomata deeply sunken (Dissanayake *et al*., 1996).

1.4.2.1.3 Phytochemical constitution

Phytochemical investigation of *F. benghalensis* led to the exploration of a wide variety of constituents that are responsible for its wide range of pharmacological activity. They include ketones, flavonoids, flavonol, sterols, oentacyclic triterpenes and triterpenoids, furocoumarin, tiglic acid ester, and some esters (Saeed *et al*., 2011). Mainly three ketones named 20-tetratriacontene-2-one, 6- heptatriacontene-10-one, and pentatriacontan-5-one were isolated from stem bark of *F. benghalensis*. These also contain flavonoids such as 5, 7 Dimethyl ether of Leucoperalgonidin-3-0-α-L-Rhamnoside and 5, 3 dimethyl ether of leucocyanidin 3-O-β-Dgalactosyl cellobioside, and 5, 7, 3 trimethoxy

leucodelphinidin 3-O-α-L-Rhamnoside. Further, leaves contain Flavonol responsible for its antioxidant effects. They also include quercetin-3-galactoside and rutin (Vikas and Vijay, 2010).

1.4.2.1.4 Antimicrobial activity

The ethanolic extraction of *F. benghalensis* showed considerable antibacterial activity against *Pseudomonas aeruginosa*, *Proteus mirabilis,* and *Bacillus cereus*. It also showed certain antibacterial effects against *Alcaligenes faecalis* and *Salmonella typhimurium* but it was inactive against *S. aureus*. Aqueous extract of *F. benghalensis* had no antibacterial activity against any of the six bacterial strains investigated above (Rathish and Sumitra, 2007). *Actinomyces viscosus* is frequently encountered in a high proportion of smooth tooth surface and gingiva. Various experiments were performed to check the antibacterial activity of *F. benghalensis* against *A. viscosus*. These showed that the extract of *F. benghalensis* bark of 0.08 mg/ml to 0.1 mg/ml has better antibacterial activity (Shandavi *et al*., 2010). Antibacterial activity of aqueous extracts of the stem bark, leaf, and root were evaluated by the agar diffusion technique. Among the three extracts, stem bark extract showed maximum antibacterial activity against *Bacillus subtilis*, *Pseudomonas aeruginosa*, *Klebsiella pneumoniae*, *Staphylococcus aureus,* and *Escherichia coli* (Ogunlowo *et al*., 2013). Thus, the methanolic extract of the stem bark of *F. benghalensis* at the dose of 200 mg/ml against Enterotoxigenic *E. coli* was highly comparable to that antibacterial activity of standard drug amikacin at the dose of 10 µg/disc (Uma *et al*., 2009).

1.4.2.2 *Ficus religiosa* (L).

1.4.2.2.1 Taxonomic Hierarchy

Kingdom: Plantae; Subkingdom: Viridiplantae; Infrakingdom: Streptophyta; Superdivision: Embryophyta; Division: Tracheophyta; Subdivision: Spermatophyta; Class : Magnoliopsida; Superorder :Rosanae; Order :Rosales; Family :Moraceae; Genus :Ficus L; Species : *Ficus religiosa* L.

1.4.2.2.2 Plant morphology

It is an evergreen or deciduous large banyan or tree, without aerial roots from the branches. Leaves are spirally arranged; new leaves are pink. Glabrous except for the sericeous or puberulous stipules and basal bracts. Twigs 3-4 mm thick. Stipules -15 mm, but larger on opening shoots. Lamina 7-26 × 4-16 cm, ovate-cordate or ovate with truncate base, caudate-acuminate with the tip 25-90 mm long, thinly coriaceous, smooth, edge often uneven or sinuous; lateral veins 6-9 pairs at a wide-angle, usually with several zigzag and obscure intercostals; basal veins 2 (-3) pairs; petiole 35-130 mm long, mostly longer than the lamina, articulate but, in some cases, rather obscurely. Figs axillary, paired, sessile, ripening pink, purple, and black; basal bracts 3, 3-5 mm long, ovate-obtuse, silky-puberulous, glabrescent; body 8-11 mm wide (10-15 mm, living), sub globose, the orifice closed by 3 apical bracts in a disc 2-3 mm wide; internal bristles none. Male flowers ostiolar, sessile in one ring; tepals 2, reddish, free, ovate-lanceolate. Gall- and female flowers sessile; tepals 3-4, red, free, short; ovary yellowish to ochraceous, red-brown at the apex or in the upper half, sessile or with a stalk -1.5 mm long, somewhat indurate and sub-angular. Lamina with cystoliths only on the lower side; stomata superficial (Dissanayake *et al*., 1996).

1.4.2.2.3 Phytochemical constitution

Phytochemicals such as phenols, tannins, steroids, alkaloids and flavonoids, β-sitosterol-D-glucoside, vitamin K, n-octacosanol, methyl oleanolate, lanosterol, stigmasterol, lupin-3-one are reported from the stem bark of *F. religiosa* (Sheetal *et al*., 2008). The fruits of *F. religiosa* contain natural flavonols namely quercetin, myricetin, and kaempferol. Also, it contains significant amounts of total flavonoid, total phenolic contents, and linoleic acid (Enit *et al*., 2018).

1.4.2.2.4 Antimicrobial activity

Antibacterial effect had been proven by using aqueous and ethanolic extracts of *Ficus religiosa* leaves against some pathogenic bacteria *Staphylococcus aureus, Salmonella paratyphi, Shigella dysenteriae, S. typhimurium, Pseudomonas aeruginosa, Bacillus subtillis,* Methicillin resistant *Staphylococcus aureus*, *Escherichia coli, Salmonella typhi* (Valsaraj *et al*., 1997). In another study, chloroform extract of fruits showed antimicrobial effect against *Azotobacter chroococcum, Bacillus cereus, Bacillus megaterium, Streptococcus faecalis, Streptomycin lactis, and Klebsiella pneumoniae* (Mousa *et al*., 1994).
The ethanolic extract of leaves showed an antifungal effect against *Candida albicans* (Farrukh and Iqbal, 2003). Aqueous, methanol and chloroform extracts from the leaves of *F. religiosa* were completely screened for antibacterial and antifungal activities. The chloroform extract of *Ficus religiosa* possessed a broad spectrum of antibacterial activity and the methanolic extracts showed moderate antibacterial activity against a few bacterial strains while there was less antibacterial activity or none at all using aqueous extracts (Hemaiswarya *et al*., 2009).

An acetone, methanol, and ethyl acetate extracts of the bark powder of *Ficus religiosa* have been checked for antibacterial activity against some medically important bacteria *Pseudomonas aeruginosa, Escherichia coli, Proteus vulgaris, Bacillus subtilis,* and *Staphylococcus aureus*. The antimicrobial assay performed by agar disc diffusion method has shown that methanol extracts had activity against *B. subtilis, E. coli, P. vulgaris, S. aureus* whereas acetone extracts showed more antibacterial activity only against *B. subtilis and E. coli* and the ethyl acetate extracts had no activity against any of the tested bacteria (Manimozhi *et al*., 2012).

1.4.2.3 *Ficus racemosa* (L).

1.4.2.3.1 Taxonomic Hierarchy

Kingdom: Plantae; Subkingdom: Viridiplantae; Infrakingdom: Streptophyta; Superdivision: Embryophyta; Division: Tracheophyta; Subdivision: Spermatophyta; Class: Magnoliopsida; Superorder: Rosanae; Order: Rosales; Family: Moraceae; Genus: Ficus L; Species: *Ficus racemosa* L.

1.4.2.3.2 Plant morphology

It is a large tree -30 m high, buttressed, occasionally deciduous, the crown often irregular and shabby; bark pinkish-brown, smooth then coarsely flaky; latex copious, cream buff. Young shoots and figs finely white hairy, soon glabrous; young leaves pale green. Twigs are 1.5-3 mm thick. Stipules -12 mm long, -30 mm long on opening shoots, often persistent on young twigs. Lamina 6-19 × 3.5-8.5 cm, elliptic varying subovate, shortly oblong or somewhat lanceolate, tapered to a subacute or sub acuminate apex, base broadly to narrowly cuneate, rarely subcordate, sub coriaceous, smooth, entire (dentate in saplings); lateral veins 4-8 pairs, -7 intercostals slightly raised below; basal veins 1 pair, short, often with a slight axillary gland; petiole 15-70 mm long, becoming brown scurfy. Figs in large clusters on the main branches and trunk, on branching leafless twigs -25 cm long, 2.5 cm thick at the base, ripening rose-red; peduncle 3-12 mm long, stout; basal bracts 1-2 mm long, ovate-triangular, obtuse; pedicel 0-5 mm long; body 20-30 mm wide (35-50 mm, living), sub globose to pyriform, often lenticellate-verrucose, orifice plane or slightly sunken, closed by 5-6 apical bracts; internal bristles none; sclerotic cells none in the thick, soft wall. Perianth with 3 (-4) dentate-lacerate lobes joined below, red, glabrous. Male flowers ostiolar in 2-3 rings, sessile, much compressed; stamens (1-2), rarely 3, often with an abortive ovary. Gall-flowers long-stalked; ovary dark red; style short. Female flowers sessile or very shortly stalked among the gall-flowers; ovary sessile or sub stipitate, red-spotted; style 2-3 mm long, glabrous, simple. Seed 1 mm long,

lenticular, smooth, not or scarcely keeled. Lamina with cystoliths present only on the lower side (Dissanayake *et al*., 1996).

1.4.2.3.3 Phytochemical constitution

The stem bark contains steroids, alkaloids, tannins (Rao Ch *et al*., 2008), glycol acetate, leucocyanidin-3-O-β-D-glucopyranoside, lupeol, friedelin, β-sitosterol, β-sitosterol-D-glucoside, gluanol acetate, quercetin, behenate, stigmasterol leuco pelargonidin-3-O-β-D-glucopyranoside, leucopelargonidin-3-*O*-α-L-rhamnopyranoside, Bergenin, racemosic acid, ceryl behenate, lupeol acetate, α-amyrin acetate (Faiyaz and Asna, 2009). The leaves contain triterpenoids, tannins, kaempferol, rutin, arabinose, bergapten, psoralenes, flavonoids, ficusin, coumarin, phenolic glycosides (Mandal *et al*., 1999). Fruits are reported to contain sterols, triterpenoids, flavonoids, glycosides, tannins, carbohydrates β-sitosterol, gluanol acetate, hentriacontane, tiglic acid of taraxasterol, lupeol acetate, gallic acid, ellagic acid, and α-amyrin acetate (Faiyaz and Asna, 2009).

1.4.2.3.4 Antimicrobial activity

Several studies have reported the antibacterial potential of *F. racemosa* against different bacterial strains. Ethanol extract of its stem bark was found to be significantly effective against *Pseudomonas aeruginosa, Proteus mirabilis, Staphylococcus aureus, Bacillus cereus, Alcaligenes faecalis,* and *Salmonella typhimurium* bacterial strains, indicating the scope to discover bioactive natural products that may serve as leads in the development of new pharmaceuticals to address unmet therapeutic needs (Nair and Chanda, 2007). In another study, the same authors reported that the ethanol extract of stem bark exhibited significant antibacterial activity against *Pseudomonas aeruginosa*, *Proteus mirabilis*, and *Bacillus cereus* bacterial strains, while the aqueous extract inhibited *Streptococcus faecalis* significantly (Nair and Chandana, 2006).

1.4.2.4 *Thespesia populnea* (L.) Sol. ex Correa

1.4.2.4.1 Taxonomic Hierarchy

Kingdom: Plantae; Subkingdom: Viridiplantae; Infrakingdom: Streptophyta; Superdivision: Embryophyta; Division: Tracheophyta; Subdivision: Spermatophyta; Class: Magnoliopsida; Superorder: Rosanae; Order: Malvales; Family: Malvaceae; Genus: Thespesia Sol. ex Correa; Species: *Thespesia populnea* (L.) Sol. ex Correa

1.4.2.4.2 Plant morphology

It is a small tree or shrub, 4-10 m or taller; twigs densely covered by small, brown, or silver scales, glabrescent. Leaves: lamina 6-13(-20) × 5.5-13 cm, deltoid, suborbicular to broadly ovate, cordate to cordate-truncate at base, long or short acuminate apex, entire, 7-veined from the base, sparsely lepidote above, more densely so beneath, glabrescent, small, saccate, extrafloral nectarines present between bases of veins beneath, not on midrib; petiole 5-8(-10) cm long, densely lepidote. Flower's axillary, solitary, large. Pedicel 2-8.5 cm long, accrescent to c. 12.5 cm, articulate at or up to 1.5 cm above base with discoid hypanthium at apex c. 1 cm diameter, lepidote, glabrescent. Epicalyx segments 3, 4-15 × 2 mm, oblong, acute, densely lepidote, caducous. Calyx 12-18 mm diameter, 8-10 mm tall, cupular, with 5-minute teeth or almost totally entire, coriaceous, accrescent to c. 25 mm diameter, and almost flattened by fruit when mature, densely lepidote without. Corolla campanulate, petals 6-7 × 4.5-6 cm, yellow maturing orange, dark-purple at the base, obovate, apex rounded. Staminal column 2.5 cm long, glabrous; filaments c. 4 mm long; anthers c. 1.5 mm long. Ovary 8-10 mm diameter, globose to ovoid, 10-celled, each cell with 4 ovules. Style c. 4 cm long. Capsule 2-4.5 cm diameter, globose, obscurely 5-angled, apex obtuse, shortly mucronate, lepidote, glabrescent, indehiscent. Seeds 9 × 6.5 mm, are obovoid to somewhat navicular, subangular or ridged, minutely short rusty pubescent to glabrous (Dissanayake *et al*., 1996).

1.4.2.4.3 Phytochemical constitution

The major phytochemical constituents reported in *T. populnea* are included Anthraquinone glycosides, cardiac glycosides, flavonoids, alkaloids, and tannins. Gossypol was found to be a major constituent producing an anti-inflammatory effect in as well as human beings (Suvarna *et al*., 2018). flowers of *T. populnea* contain kaempferol, β-sitosterol, gossyptein and a mixture of Kaempferol 3-glucoside, Quercetin 3-glucoside, Kaempferol 5-glucoside separated, Rutin, Kaempferol 3-rutinoside and Kaempferol 7-glucoside (Datta *et al*., 1973). Dextro-rotatory gossypol has recently had been isolated from flowers, fruits, and bark (Suvarna *et al*., 2018). Heartwood is reported to contain sesquiterpenoids, named Populene A-H (1-8). It also contains six Sesquiterpenoidal quinones of the mansonone group containing the cadalene skeleton. Four were identified as Mansonone C, D, E, and F. The other two are new natural products belonging to this group and are named thespesone I and thespone II (Neelakantan *et al*., 1983). The stem bark contains alkaloids, carbohydrates, protein, tannins, phenols, flavonoids, gums and mucilage, saponins, terpenes, as well as β-Sitosterol-3-O- β-D-glucopyranoside-6'-O-stearate, β- Sitosterol, Daucosterol, Kaempferol, 1-Hentriacontanol, Stearic acid, Betulin (Vasudevan *et al*., 2007).

1.4.2.4.4 Antimicrobial activity

Antibacterial and antifungal activities of *T. populnea* leaf extracts (hot and cold) have been studied using seven solvents (hexane, chloroform, dichloromethane, ethyl acetate, acetone, methanol, and water) against human pathogens. Antibacterial and Antifungal activities of crude extracts were determined by the disc diffusion method. The highest antibacterial activity was exhibited by methanol cold extract against *Staphylococcus epidermidis* and *Bacillus cereus* respectively. Hot hexane extract showed inhibition against *Pseudomonas aeruginosa*. Both the cold and hot extracts of all the seven solvents exhibited inhibition zones against *Candida albicans* (Pratap *et al*., 2014). Ethanolic and aqueous root extracts of *T. populnea* were checked for dose-dependent antibacterial activity. *Thespesia populnea* showed broad-spectrum antimicrobial activity against gram-positive and gram-negative bacteria and maximum inhibition by the ethanolic extract was observed at the higher dose (400 mg/ml). The results concluded that the antimicrobial activity of *T. populnea* was dose-dependent (Rajan *et al*., 2013).

1.4.2.5 *Ficus arnottiana* (Miq.). Miq.

1.4.2.5.1 Taxonomic Hierarchy

Kingdom: Plantae; Phylum: Tracheophyta; Class: Magnoliopsida; Order: Rosales; Family: Moraceae; Genus: Ficus; Species: *Ficus arnottiana* (Miq.) Miq.

1.4.2.5.2 Plant morphology

It is a small deciduous banyan or independent tree to 10 m high, without aerial roots from the branches; bark grey-brown. Leaves spirally arranged; veins and petioles bright pink; new leaves brownish-pink. Glabrous. Twigs 3-5 (-6) mm wide. Stipule 12-40 mm long, glabrous, caducous, -6 cm and leafy on young shoots. Lamina 6-14 × 5-9 cm (-25 × 14.5 cm in saplings), ovate-cordate, rarely short-ellipsoid, acuminate with a tip -22 mm long (-40 mm in sapling), base deeply cordate, entire, thinly to rather thickly coriaceous, undulate, drying dull greyish-brownish, smooth; lateral veins 5-7 pairs (-10 in saplings), scarcely raised below, venation as in F. religiosa; basal veins 2-3 pairs, the larger pair 1/3-1/2 lamina; petiole 30-70 mm (-170 mm in sapling), not articulate. Figs in axillary pairs and on the twigs below the leaves, glabrous, ripening yellow-brown, red (?) or purple with green spots (King); peduncle 2-5 × 1 mm: basal bracts 3, 1 × 2-2.5 mm, blunt, thin, eventually caducous; body 5-8 mm wide, globose, not pedicellate, orifice small, plane; internal bristles none. Tepals red, glabrous, rather fleshy, gamophyllous, the perianth 3-4 lobed. Male flowers sessile, round the orifice and sparsely scattered in the interior of fig; stamen 1. Gall- and female flowers sessile or shortly stalked; ovary

sessile, straw-white with a slight red patch on the stylar side; style slender. Lamina with cystoliths presents on both sides; stomata superficial; cuticle slightly striate round stomata (Dissanayake *et al*., 1996).

1.4.2.5.3 Phytochemical constitution

Preliminary phytochemical screening: It was found that ethyl acetate, methanol, and aqueous extracts of *Ficus arnottiana* leaves contained tannins, flavonoids, saponins, triterpenoids, steroids, glycosides, anthraquinones, reducing sugars, carbohydrates, proteins, and amino acids (Gurpreet and Satnam, 2016).

1.4.2.5.4 Antimicrobial activity

Ethyl acetate, methanol, and aqueous extraction of leaves of *Ficus arnottiana* were tested against two Gram-positive (*Staphylococcus aureus, Bacillus subtilis*) and two Gram-negative (*Escherichia coli, Pseudomonas aeruginosa*) human pathogenic bacteria as well as two fungal species (*Fusarium solani* and *Candida albicans*). The results showed that a remarkable inhibition of the bacterial growth was shown against the tested organisms. Ethyl acetate extraction showed maximum antimicrobial activity against *S. aureus* in 200 µg/ml concentration while methanol extraction showed less antimicrobial activity. Aqueous extraction showed a good antimicrobial result in almost all microbial strains at a concentration of 200 µg/ml. Thus, acetate and methanolic extract do not show antimicrobial activity against *E. coli* and *P. aeruginosa*. Aqueous extract has shown more antifungal activity as compared to the methanolic extract. Also, the methanolic extract has not shown any antifungal activity against *Candida albicans* (Gurpreet and Satnam, 2016).

1.4.2.6 *Abutilon indicum* (L.) Sweet.

1.4.2.6.1 Taxonomic Hierarchy

Kingdom: Plantae; Subkingdom: Viridiplantae; Infrakingdom: Streptophyta; Superdivision: Embryophyta; Division: Tracheophyta; Subdivision: Spermatophyta; Class: Magnoliopsida; Superorder: Rosanae; Order: Malvales; Family: Malvaceae; Genus: Abutilon Mill; Species: *Abutilon indicum* (L.) Sweet.

1.4.2.6.2 Plant morphology

It is a woody herb or subshrub, erect, 0.3 (-1.5) m tall, slightly branched, densely pubescent especially on young stems. petioles and pedicels with dense stellate indumentum, intermixed or not with fine, long, white, patent hairs. Leaves: lamina 2.5-5 × 2-5 cm, ovate to ovate-lanceolate or suborbicular, obtuse to acute, rarely acuminate, base obtuse to cordate, serrate-dentate, sub scabrid above, velvety beneath, palmately 5-7-veined, veins prominent beneath; petioles 0.5-5 (-12.5) cm long, tomentose; stipules 2-3 mm long, linear to filiform, obscure, early deciduous. Flower's solitary, axillary, up to c. 3 cm diameter, yellow to orange-yellow, lacking a purple center. Pedicels 2-5 cm long, accrescent to 8 cm, stout, joint above, tomentose. Calyx campanu1ate 5-11 mm long, c. 10-12 mm diameter, lobes 3.5-8 x 3-5 mm, broadly ovate to triangular, densely ste1late-pubescent without, woolly-hairy within, eventually spreading to sub reflexed at maturity. Petals 1-1.75 cm long, overlapping, longer than calyx. Staminal column 5-7 mm long, stellate-pubescent. Schizocarp globular, 1.5-2 cm diameter. Mericarps 15-20, white-hairy with long-stellate and simple hairs, c. 2-4 times length of CA: Of calyx, apically long-acute or acuminate, not beaked. Seeds c. 3, 1-1.5 mm reniform, grey to pale-brown, glabrous, moderately to sub densely lepidote with minute raised scales (Dissanayake *et al*., 1996).

1.4.2.6.3 Phytochemical constitution

Phytochemical constituents from the root contain non-drying oil which consists of different fatty acids like linoleic, oleic, stearic, palmitic, lauric, myristic, caprylic, capric have been reported (Rajurkar *et al*., 2009). Different types of flavonoids such as Quercetin-3-O-β-D-glucopyranoside, Luteolin-7-O-β-glucopyranoside and Quercetin-3-O-α-rhamnopyranosyl (1-6)-β-glucopyranoside have been isolated from an

extract of this flower (Matlawska *et al*., 2002). The leaf extract of *A. indicum* (L) Sweet consists of various steroids such as β sitosterol, cholesterol, and stigmasterol (Macabeo and Lee, 2014; Rahuman *et al.*, 2008). Quercetin is an important flavonol found in leaf extract of *A. indicum* (Rajput and Patel, 2012). Thus, certain flavones have been observed from this plant like Luteolin, Luteolin-7-O-β-glupyranoside, Chrysoeriol-7-O-β-glupyranoside, and Chrysoeriol (Singh and Gupta, 2008).

Mucilaginous substances, asparagine, saponins, flavonoids, alkaloids have been isolated from the whole plant (Sharma *et al*., 2013). There is the presence of various sterols β-Sitosterol, β-Sitosterol-3-O-β-D-glucopyranoside along with phenolic acid derivatives Benzoic acid, Hydroxybenzoic acid, Stigmasterol, Benzoic acid, Caffeic acid, 4-Hydroxyacetophenone, 4-Hydroxybenzaldehyde, Vanillin, and Syringaldehyde. The phytochemical screening of whole extracts of *Abutilon indicum* showed the presence of β-sitosterol-3-O-β-D-glucopyranoside as sterols, and also some phenolic acid derivatives (Venkat and Suvarna, 2020).

1.4.2.6.4 Antimicrobial activity

A new steroidal compound 20, 23-dimethyl cholesta-6, 22- dien-3β-ol has been isolated from the stem tissues of *A. indicum*. The structure of the compound has been elucidated by spectral and chemical studies. The compound was found to be 100% effective at 5000 ppm in controlling the mycelial growth of *Aspergillus terreus var. aureus* and *Aspergillus parasiticus var*. *globosus* using the poison food technique (Prabhuji *et al*., 2010). Chloroform, ethanol, and aqueous extracts of the leaves of *A. indicum* have been investigated for antibacterial activity against *Staphylococcus aureus, Bacillus subtilis, Klebsiella pneumoniae, Salmonella typhi, Escherichia coli,* and *Pseudomonas aeruginosa*. Among the various extracts maximum antibacterial activity has been exhibited by ethanol extract followed by chloroform extract while aqueous extract has not shown activity (Reyad -Ul *et al*., 2015).

1.4.2.7 *Garcinia quaesita* Pierre

1.4.2.7.1 Taxonomic Hierarchy

Kingdom: Plantae; Clade: Tracheophytes; Clade: Angiosperms; Clade: Eudicots; Clade: Rosids; Order: Malpighiales; Family: Clusiaceae; Genus: Garcinia; Species: *Garcinia quaesita* Pierre.

1.4.2.7.2 Plant morphology

It is a tree, up to 20 m tall, up to 60 cm diameter, glabrous in all its parts. Bark is rough, dark rusty to blackish, cracked and peeling off in rectangular 1–1.5 cm wide, 2 mm thick pieces; live bark 5–10 mm thick, outer part brown-red, inner one yellowish, with thick, sticky, dark yellow latex. Branchlets are slender, cylindrical with a raised, slender ring at the nodes. Leaves chartaceous to firmly chartaceous (dried), oblanceolate to sub obovate or elliptic, 3.5 × 12– 1.5 × 6–5 × 10 cm, obtuse or shortly acutish or with a broad, very short acumen, base tapered, acute, slightly decurrent into the slender, 1–1.5 cm long petiole, foveola inconspicuous. Laterals 8-10 pairs with as many, almost as long parallel ones in between, rather erect (narrow leaves) or erect-patent, slender, promiscuous both surfaces, reticulation very lax; midrib flat in its basal part on the upper surface, slender, prominent, reddish-brown on the lower one. Flowers are white, male ones fascicled in the axils of the upper leaves, pedicels up to 2 cm long, slender, slightly thickened at the apex, outer 2 sepals spreading, concave, oblong-orbicular, stiff, thick, 2 mm long; inner two erect, oblong, 3–3.5 mm long. Petals 4–5 fleshy, ovate to elliptic, acutish, 5-7 mm, base often narrowed. Stamens connate into a cylindrical, 1–1.5 mm long column, bearing the c. 10 anthers on 0.5 mm long free part of filaments. Female flowers solitary and pseudo-terminal, pedicel 2–5 mm long, sepals up to 5 mm long (in fruiting stage). Free stamens as many as grooves of the ovary, filaments slender, up to 3 mm long, anthers 0.5 mm long; ovary with 6-9 grooves, crowned by a sessile, dome-like stigma with rays of papillae, obscurely separated, only incised at the margin. Fruit is globose to sub-ovoid, up to 5 cm diam., red to orange-red, glossy with 6-9 very deep

grooves and as many ribs, running to the tip of the fruit and there curving inwards into an up to 1.5 cm deep depression, from which center arises a thick, cylindrical, up to 2 cm long mamilla, of which the flat top is the obscurely rayed, papillate stigma, 2-4 mm in diam., incised only at the margin, the persistent sepals reflexed under the fruit (Dissanayake *et al*., 1996).

1.4.2.7.3 Phytochemical constitution

Garcinia quaesita is a plant species endemic to Sri Lanka and there are a few studies conducted for its phytochemical analysis. Garcinol which has high antioxidant properties is the main active chemical compound that can be found in *G. quaesita* fruit as well as leaves (Rajapaksa *et al*., 2020). Although the phytochemical composition of this plant has not been properly studied it is rich in acid and possesses marked antiseptic properties. Thus, it contains tartaric acid 10.6 %, reducing sugar as glucose (15%) and phosphoric acid as calcium triphosphate. Pectin has also been isolated from fruits as well as 16.3% of hydroroyl citric acid (HCA) (Sawade and Tomi, 1997). The bark of the *G*arcinia *quaesita* mainly contains quaesitol, Phenolic compounds, Hermon ionic acid, and also its decarboxylated product (Gunathilake *et al*., 1984). Furthermore, another study revealed that number of phytochemical compounds such as phenols, flavonoids, alkaloids, saponins, steroids, and terpenoids were present in higher amounts in water extracts of *G. quaesita* fruit (Hewageegana *et al*., 2018).

1.4.2.7.4 Antimicrobial activity

The antibacterial activity of 21 nm TiO_2 nanoparticles and particles modified with *Garcinia zeylanica* (*G. quaesita*) against Methicillin-resistant *Staphylococcus aureus* had been investigated in the presence and absence of light. Surface modification of TiO_2 NPs with the adsorption of *G. zeylanica* extract caused a shift of the absorption edge of TiO_2 NPs to a higher wavelength. TiO_2 NPs, *G. zeylanica* pericarp extract showed significant bactericidal activity which was further enhanced in contact with the TiO_2 modified *G. zeylanica* extract.

The antimicrobial activity was enhanced in the presence of TiO_2 NPs modified with *G. zeylanica* and with a longer contact time (Senarathna *et al*, 2017). Aqueous and ethanolic extracts of *G. quaesita* showed inhibition against *Escherichia coli* and *Staphylococcus aureus* while no antifungal activity was observed against *Candida albicans* (Alwis *et al.,* 2021). Methanolic extracts of *G. zeylanica* was prepared from the dried fruit rind and leaves to be tested for their antimicrobial effect against 5 bacterial species (*Escherichia coli*, *Staphylococcus aureus*, methicillin-resistant *Staphylococcus aureus* (MRSA), *Pseudomonas aeruginosa,* and *Streptococcus pyogenes*) and yeast (*Candida albicans*) using agar well diffusion method. The overall results of the antimicrobial assay have provided promising primary information for the potential of using crude extract of the dried fruit rind of *G. zeylanica* in the treatment of infections caused by both tested bacteria and fungi (Nirasha *et al*., 2019).

A study had biosynthesized stable silver nanoparticles (Ag-NPs) from *Garcinia zeylanica* crude aqueous extract and 95% pure garcinol. Not only that, their antimicrobial activity was also investigated. The antimicrobial activity of synthesized Ag-NPs was tested against *Pseudomonas aeruginosa*, *Escherichia coli*, *Staphylococcus aureus,* and *Candida albicans* by well diffusion method. The mean zones of inhibition (ZOI) of small Ag-NPs against *E. coli*, *P. aeruginosa*, *S. aureus,* and *C. albicans* were 12.6 mm, 13 mm, 11 mm, and 10.66 mm, respectively. The mean ZOI of large Ag-NPs against the above organisms was 11 mm, 10.66 mm, 10 mm, and 10 mm, respectively and the result indicated that antimicrobial activity of Ag-NPs decreased with their increasing particle size (Wijekoon *et al*., 2017).

1.4.2.8 *Chrysophyllum cainito* L.

1.4.2.8.1 Taxonomic Hierarchy

Kingdom: Plantae; Subkingdom: Viridiplantae; Infrakingdom: Streptophyta; Superdivision: Embryophyta; Division: Tracheophyta;

Subdivision: Spermatophyta; Class: Magnoliopsida; Superorder: Asteranae; Order: Ericales; Family: Sapotaceae; Genus: Chrysophyllum L; Species: *Chrysophyllum cainito* L.

1.4.2.8.2 Plant morphology

An evergreen tree, conforming to Troll's architectural model, is up to 30 m tall with white gummy latex. Branchlets are numerous, plagiotropic brown hairy, glabrescent; the upright basal parts of successive leading branches align to form the trunk. Leaves are alternate, spreading, oblong to obovate, 5-16 cm × 3-6 cm, leathery, reddish ferruginous-sericeous on both sides, quickly glabrescent above, almost parallel secondary nerves very characteristic; Petioles 0.6-1.7cm long. Inflorescence's axillary on current season's shoots with 5-35 clustered, small, yellowish to purplish white color flowers; sepals -5, circular to ovate; corolla tubular, ca.4mm long, lobes5, ovate; stamens 5; stigma 7-10 lobed. Fruit is an obovoid-globose berry, 5-10 cm in diameter, purplish-brown or yellowish-green, skin thin, glossy, glabrous, leathery, flesh purple or white,3-12mm thick, soft and juicy, surrounding the 4-11-celled endocarp, which is start-like when cut transversely. Seeds are about 3-10, flattened obovoid, about 2 cm × 1 cm × 0.5 cm, purplish-black, with chartaceous testa and a large lighter-colored hilum.

1.4.2.8.3 Phytochemical constitution

The extracts of different parts of *C. cainito* contain phenols, alkaloids, flavonoids, steroids, saponins, tannins, and cardiac glycosides found in the stem bark (Doan *et al*., 2018). It was found that the leaves of *C. cainito* contain gallic acid, galloyl myrecetrin, rutin, quercetrin, myrecetrin, myricetin, quercetin, and two triterpenoids *β*-amyrin and lupeol, ursolic acid, β-sitosterol, lupeol, and gallic acid (Sayed *et al*., 2019). It was reported nine characterized flavonoids from *C. cainito* fruit including (+)-catechin, (–)-epicatechin, (+)-gallocatechin, (–)-epigallocatechin, quercetin, quercitrin, isoquercitrin, myricitrin, and gallic acid and both green and ripe fruits contain vitamin C, phenolic compounds, and flavonoid compounds (Kubola *et al*., 2011).

1.4.2.8.4 Antimicrobial activity

The seed and pulp of *C. cainito* have exhibited varying levels of antibacterial and antifungal activities using agar well diffusion method against some clinical isolates such as *Staphylococcus aureus*, *Escherichia coli*, *Salmonella typhi*, *Pseudomonas aeruginosa*, *Candida albicans*, *Aspergillus*, and *Penicillium ascomycetous* fungi. The water extract was more sensitive to *Staphylococcus*, *Pseudomonas*, and *Salmonella* (Oranusi *et al*., 2015). The green synthesis of silver nano/microparticles of a leaf extract from star apple combined with leaf extract from mango inhibited the growth of *Staphylococcus aureus* (Lagbas *et al*., 2016) and interestingly, the peels of *C. cainito* exhibited significant antiviral activity. Antiviral activity of peels of *C. cainito* has been demonstrated through HIV-1 RT inhibition using a nonradioactive immuno/colorimetric assay (Guerrero *et al*., 2018).

1.4.3 Literature review of silver nano/ionic particles

1.4.3.1 Green synthesis and monitoring of silver nanoparticle

The primary requirement of green synthesis of Ag-NPs is silver metal ion solution and a reducing biological agent. In most cases, reducing agents or other constituents present in the cells act as stabilizing and capping agents, so there is no need of adding capping and stabilizing agents from outside. The Ag^+ for the synthesis of Ag-NPs can be obtained from various water-soluble salts of silver, the aqueous $AgNO_3$ solution with Ag^+ concentration range between 0.1 – 10 mM (usually 1mM) has been used commonly. The appearance of color changes has been taken as indicative of Ag-NPs synthesis by almost all scientists. The SPR (Surface plasmon Resonance) peak of the synthesized Ag-NPs was witnessed;

the range of 400 - 450 nm is the significant range for Ag-NPs (Sastry *et al*., 1997).

1.4.3.2. Mechanism of green synthesis of silver nanoparticles

The synthesis of silver nanoparticles by biological entities is due to the presence of many organic chemicals like carbohydrates, fat, proteins, enzyme, and coenzymes, and other phytochemicals like phenols, flavonoids, alkaloids, gum, etc. which are capable of donating electrons for the reduction Ag^{+} to Ag^{0}. The active ingredient responsible for the reduction of Ag^{+} varies depending upon the organism/extract used. For nano- transformation of silver nanoparticles, electrons are supposed to be derived from dehydrogenation of acid (ascorbic acid) and alcohol (catechol) in hydrophytes, keto to enol conversions (cyperaquinone, dietchequinone, remirin) in mesophytes or both mesophytes or both mechanisms in xerophytes plants. The microbial cellular and extracellular oxidoreductase enzymes can perform similar reduction processes (Jha *et al*., 2009).

1.4.3.3 Antibacterial mechanism of silver nanoparticles

The antibacterial properties of Ag-NPs mainly depend upon the size, pH, and ionic strength of the medium, surface charge, dosing, and diffusion state, and also on the type of capping agent. However, the specific mechanism of antibacterial or toxicity activities by the Ag-NPs is still indefinite and has not been completely explained. Sometimes, the Ag-NPs could frequently release the silver ions (Ag^{+}), which might be considered as one of the mechanisms behind the bactericidal activity of Ag-NPs (Bapat, *et al*., 2018). Apart from the ability to release the Ag^{+} ions, the Ag-NPs could themselves eradicate the microbes or bacteria. The amassed Ag-NPs trigger denaturation of the cell membranes and due to the size of the nanoscale they can permeate through the cell wall of bacteria and consequently modify the cell membrane arrangements (Liao *et al*., 2019).

The organelles might get ruptured due to denaturation of the cell membrane, and it might cause cell lysis. Also, the Ag-NPs could be included in microbial signal transduction. The microbial signal transduction is impacted by the phosphorylation of protein substrates, and the Ag-NPs could potentially dephosphorylate the tyrosine residuals over the peptide substrates. Furthermore, the disruption of microbial signal transduction could significantly cause cell apoptosis and inhibition of cell propagation. The antibacterial efficacy and mechanism of the Ag-NPs are affected by their dissolution profile in the reaction media. The dissolution efficacy is highly dependent upon the synthesis and processing parameters, including intrinsic characteristics of Ag-NPs and the dissolution media (Noronha *et al*., 2017).

Apart from these, the size and shape of the Ag-NPs influence the production of Ag^{+} ions and this phenomenon is described theoretically by the Ostwald–Freundlich equation. According to it, the Ag-NPs having small size and sphere-shaped or quasi-spherical arrangement are more susceptible to the release of Ag^{+} ions owing to their greater surface area (Shanmuganathan, *et al.*, 2018). Thus, the surrounding media also influences the release of Ag^{+} ions. The existence of organic or inorganic constituents in the surrounding media affects the dissolution of Ag-NPs by accumulating with Ag-NPs or forming complexes with the Ag^{+} ions. Moreover, as compared to the neutral media, the Ag-NPs release the Ag^{+} ions more rapidly in the acidic media (Jacob *et al*., 2019).

Previous investigations have shown that Gram-negative bacteria are more liable to Ag-NPs than Gram-positive bacteria. There is a more tapered cell wall in Gram-negatives as compared to Gram-positive bacteria. The thick cell wall decreases the diffusion of the Ag-NPs into the cellular environment of Gram-positive bacteria. The diverse antibacterial activities of Ag-NPs over the Gram-negative and Gram-positive bacteria suggested that the uptake of Ag-NPs is essential for effective antibacterial or antimicrobial action (Noronha *et al*., 2017).

However, Gram-positive pathogens are composed of very thick cell walls composed of various peptidoglycan coats, thus serving as a barrier for the permeation of the Ag^+ ions through cytoplasmic membranes. However, gram-negative pathogens mostly consist of only a single peptidoglycan coat, thus Ag^+ ions easily penetrate the cytoplasm and cause cell lysis.

Apart from that, it has been recognized that Ag-NPs smaller than 10 nm could directly modify cell penetrability, go into the bacterial cells and initiate cell lysis (Saravanan *et al*., 2018). Apart from these, as per the reported studies, the inhibition of both protein synthesis and cell wall synthesis are triggered by Ag-NPs and they are evidenced by the amassing of envelope protein precursor or disruption of the outer cellular membrane, leading to ATP leakage (Park *et al*., 2011).

1.4.3.4 Toxicity of silver nanoparticles

The silver nanoparticles have played a crucial role in different fields of biomedical and pharmaceutical applications. The smaller size of the Ag-NPs allows easy passage through the biological membranes and reaches within the cells, producing toxicity at various levels based upon the increased microorganisms. The toxicity of the Ag-NPs is found to be associated with its features like size, shape, amount, accumulation, surface charge, and the methods applied for synthesis (Akter *et al.*, 2018). Apart from that, the toxicity of Ag-NPs depends upon the category of targeted microbe which is attached with the resistance mechanism of the microbe that is used to eradicate the unwanted complexities (Hussain *et al*., 2019).

1.4.3.5 Antibacterial mechanism of silver ion

Silver-based antimicrobials can be effective in the treatment of infections as their non-toxicity of active silver ions (Ag^+) to human cells (Ewald *et al*., 2006). The mechanism of antimicrobial action is closely related to their interaction with thiol (sulfhydryl) groups. Mainly some amino acids such as cysteine, as well as some other compounds like sodium thioglycolate containing thiol groups neutralize the activity of silver against bacteria (Liau *et al*., 1997). However, disulfide bonds containing amino acids, non - sulfur-containing amino acids, as well as sulfur-containing compounds (cystathionine, cystic acid, sodium bisulfate, etc.,) are unable to neutralize the activity of silver ions.

Silver ions particularly inhibit these thiol group-containing enzymes, such as NADH dehydrogenase II and increase the production of free radicals. The increment of catalase production in the presence of ROS could be explained by the necessity for cells to reduce the concentration of H_2O_2, which is the source of the free radicals. It is proposed that ROS can induce the apoptotic pathway in bacteria which could ultimately lead to their death. Thus, at a lower concentration of silver nitrate, respiratory nitrate reductase may be involved in the production of nanoparticles that can cause cell death but at higher concentration, silver nitrate inhibits the action of proteins by reacting with their thiol groups and also binds with DNA, thus arresting the replication (Matsumura *et al*., 2003).

02- Methodology

2.1 Type of the study

This was a laboratory-based *in vitro* experimental study. The study was carried out at the analytical chemistry laboratory of the Postgraduate Institute of Science, and the Microbiology laboratory of the Faculty of Dental Sciences, University of Peradeniya. Scanning electron microscopy was done at the Department of Geology, Faculty of Science, University of Peradeniya.

2.2 Authentication of plants and naming of the *Panchavalkala* combinations

First of all, each plant that was included in *Panchavalkala* combinations was authenticated from the herbarium of the Royal Botanical Garden, Peradeniya, Sri Lanka. Three combinations of Panchavalkala selected for study were named as A, B, and C as mentioned in the table 2.1.

Table 2.1: Medicinal plants included in the *Panchavalkala* combination.

A	B	C
Ficus benghalensis	*Ficus benghalensis*	*Ficus benghalensis*
Ficus racemosa	*Ficus racemosa*	*Ficus racemosa*
Ficus religiosa	*Ficus religiosa*	*Ficus religiosa*
Ficus arnottiana	*Thespesia populnea*	*Chrysophyllum cainito*
Garcinia quaesita	*Abutilon indicum*	*Garcinia quaesita*

2.3 Materials and methods

2.3.1 Preparation of three *Panchavalkala* extracts

This extraction procedure was carried out according to the methods described in Sri Lankan Ayurvedic pharmacopeia for the preparation of decoctions. Mature, undamaged, and disease-free barks of each plant were taken and cleaned to remove debris and thoroughly washed using deionized water, and allowed to air dry. Plant parts were cut into small pieces and after that, 12 g of each plant material was added to a maximum weight of 60 g for each sample. Then they were cut further into small pieces and added to a 1000 ml beaker. Similarly, A, B, and C combinations were prepared separately. Afterwards, 960 ml of sterile deionized water was added and boiled up to a final volume of 120 ml (8: 1 concentration). Thus, the resulting extract was filtered using Whatman No.1 filter papers and each filtrate was obtained separately, and each sample was separately labeled, and three filtrates were stored at 4°C separately for further requirement. During each step of the extraction procedure, sterility was maintained effectively without contamination.

2.3.2 Preparation of the extract of the individual bark

A sample of 10 g of air-dried bark of each plant was weighed separately and transferred into eight 250 ml beakers, each beaker was labeled, and 100 ml of deionized water was added into each beaker and gently boiled for about 30 minutes. All extracts were then filtered through Whatman No.1 filter paper to remove particulate matter and to get clear solutions which were then refrigerated (4°C) in 250 ml Erlenmeyer flasks until further experiments. All the steps were done under sterile conditions.

2.3.3 Synthesis of Ag -NPs using *Panchavalkala* extracts

An aqueous solution (1 mM) of silver nitrate ($AgNO_3$) was prepared in a 250 ml Erlenmeyer flask. Then 10 ml of each Panchavalkala extraction were taken into 150 ml three conical flasks and labeled as A, B, and C. After that, 90 ml of 1mM solution of silver nitrate was added into each extraction separately. This setup was incubated in a dark chamber to minimize the photo-activation of silver nitrate at room temperature. The composite mixture was heated at 60 ° C for complete bio reduction for 5 min. The color of the mixture changed from the initial light yellow to light brown to reddish-brown within a maximum period of 15 minutes (Priya *et al*., 2014). This was separately performed with each Panchavalkala extract named A, B, and C. Reduction of Ag^+ to Ag^0 was confirmed by the color changes of solutions from light yellow to colloidal brown. The diluted reddish-brown solutions were cooled to room temperature and kept aside for 24 h for complete bio reduction and saturation denoted by UV- visible spectrophotometric scanning. Then, colloidal mixtures were sealed and stored properly for further use.

2.3.4 Characterization of Silver nanoparticles

2.3.4.1 Ultraviolet-visible spectroscopy analysis of silver nanoparticles

A sample of 1 ml of each of the three samples was collected periodically to monitor the completion of bio reduction of Ag^+ in aqueous solution, followed by dilution of the samples with 2 ml of deionized water and subsequent scan in UV-visible (vis) spectra, between a wavelength of 300 to 800 nm in a double beam spectrophotometer (SHIMADZU- Model No. UV1800). The deionized water was used as the blank (control).

2.3.4.2 Scanning electron microscopy (SEM) analysis

Each of the colloidal solutions containing Ag-NPs was centrifuged at 4000 rpm for 15 min, and the pellets were discarded and one drop of each supernatant of the samples was placed on a glass coverslip followed by air-drying. The coverslip itself was used during the scanning electron microscopy analysis. The samples were then gold-coated using a coater (Sputter coater, Model No. SC7620). The images of Ag-NPs as well as each Panchavalkala sample were obtained in a scanning electron microscope (ZEISS EVO-LS 15, Germany). The details regarding applied voltage, magnification used, and size of the contents of the images were implanted on the image itself.

2.3.5 Estimation of antimicrobial activity

2.3.5.1 Selection of microorganisms

The comparative antimicrobial activity of the respective extracts was effectively assessed against *Escherichia coli* (NCTC 10418), *Pseudomonas aeruginosa* (NCTC 10622), *Candida albicans* (ATCC 90028), methicillin-resistant *Staphylococcus aureus* (ATCC 43300) and methicillin-sensitive *Staphylococcus aureus* (NCTC 12384). Further ten clinical isolates each of methicillin-sensitive *Staphylococcus aureus* (MSSA) and methicillin-resistant *Staphylococcus aureus* (MRSA) were used.

The antimicrobial activity of each Panchavalkala combination named as A, B, C, and green synthesized Ag-NPs, aqueous bark extract of each eight plants were checked using the well diffusion method. Each test was quadruplicated. Commercially available fluconazole (50 µg/ml) was used as a positive control for *Candida albicans* and gentamicin (10 µg/ml) were used for *Pseudomonas aeruginosa* and *Escherichia coli* while commercially available amoxicillin (10 µg/ml) and vancomycin (30 µg/ml) were used respectively as positive controls for MSSA and MRSA. Sterile deionized (SD) water was used as negative control. Antimicrobial activity of 1 mM silver nitrate aqueous solution and plant extract without Ag-NPs also studied. Freshly cultured microorganisms on respective culture media were used for the preparation of inoculum in sterile PBS (0.5 MacFarland).

2.3.5.2 Media preparation

The Mueller Hinton Agar (MHA) medium was prepared following the instruction given by the manufacturer (OXOID CM 0337 MUELLER-HINTON AGAR). Accordingly, MHA was dissolved into water in the bottle and medium was autoclaved at 121 ℃ in 15 min.

2.3.5.3 Culture plate preparation

Each culture plate was poured with 25 ml of liquid MHA and left for solidification. Then, 3 ml of microbial inoculum (McFarland 0.5 standard solution) was pipetted onto the agar surface of the plate and equally spreader using a sterile glass spreader. After 1 min, the excess broth culture inoculum was pipetted out from the plate and allowed to dry for 3-5 minutes. Then wells (9 mm diameter) were cut on agar using a sterile cork borer. Wells were sealed with liquid MHA.

2.3.5.4 Antimicrobial assay

The samples A, B, C containing Ag-NPs, samples A, B, C without Ag-NPs, individual plant bark extract and 1 mM silver nitrate aqueous solution of each containing at the quantity level of 185µl were loaded into wells and incubated 24 hours

aerobically at 37 ℃. The same procedure was carried out using each Panchavalkala combination and Ag-NPs synthesized from each sample for ten clinical isolates of MSSA and MRSA and it was duplicated and the mean value was calculated. The mean zone of inhibition (ZOI) was calculated on a millimeter scale (Allafchian *et al*., 2016).

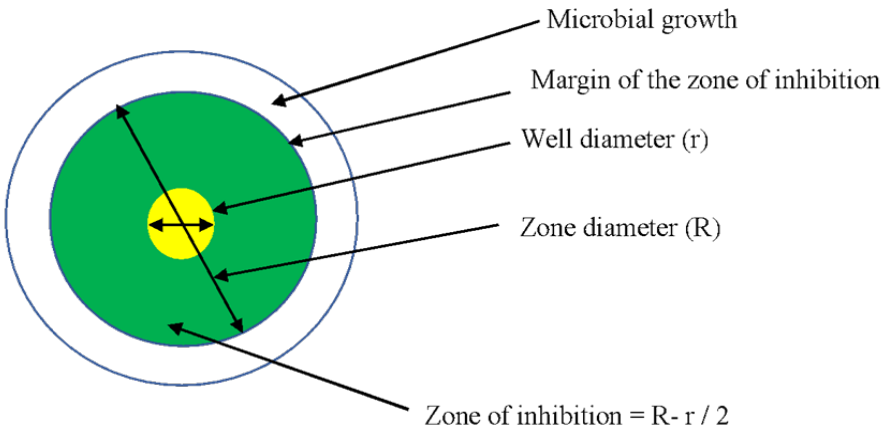

Figure 2.1 Method of calculation zone of inhibition

2.3.6 Statistical analysis

Analytical determination was done in quadruplicate which related to all experimental data. Those data were expressed as mean ± standard deviation and all the statistical analyses were carried out using SPSS - 20 version software. Statistical significance of the data was analyzed by a two-sample t-test and one-way ANOVA with a significance limit set at 5% probability. Data was represented by tabulating and using appropriate bar charts.

This study was conducted to green synthesize silver nanoparticles using water extracts of the three combinations of *Panchavalkala* and to identify its antimicrobial activity against some of the common wound pathogens. First of all, antimicrobial effects of each *Panchavalkala* combination were studied against standard bacteria followed by ten clinical isolates each of MSSA and MRSA. Antimicrobial activity of bark extracts of each plant species against the same pathogens was also studied. Finally, Ag-NPs were synthesized by using each *Panchavalkala* combination and their antimicrobial activity was identified against above microorganisms.

3 - Results and Discussion

3.1 Analysis of Antimicrobial activity

3.1.1 Antimicrobial activity of *Panchavalkala* against standard isolates of common wound pathogens

Table 3.1: Mean zone of inhibition (ZOI) of each *Panchavalkala* combination against common wound pathogens.

	Microorganism and ZOI in (mm)				
Sample	*E. coli*	*Pseudomonas*	*S. aureus*	MRSA	*Candida*
A	No ZOI	No ZOI	4.81 ± 0.26	4.69 ± 0.26	No ZOI
B	No ZOI	No ZOI	4.25 ± 0.27	3.88 ± 0.23	No ZOI
C	No ZOI	No ZOI	5.12 ± 0.23	4.50 ± 0.38	No ZOI
Gentamicin	5.38 ± 0.23	2.38 ± 0.23			
Amoxicillin			4.50 ± 0.42		
Vancomycin				4.00 ± 0.38	
SD water	No ZOI	No ZOI	No ZOI	No ZOI	No ZOI
fluconazole					4.81 ± 0.37

The above table 3.1 indicates that mean ± SD of samples A, B, and C against *Staphylococcus aureus* and MRSA were 4.81 mm ± 0.26 and 4.69 mm ± 0.26, 4.25 mm ± 0.27 and 3.88 ± 0.23, 5.12 mm ± 0.23and 4.50 mm ± 0.38 respectively. There was a significantly high inhibition $P < 0.05$ (P=0.005) of *Staphylococcus aureus* by sample C compared to amoxicillin as the control. Samples A (P = 0.001) and C (P = 0.019) showed significantly higher effect against MRSA when compared with vancomycin. There was no inhibitory effect of sample A, B and C on Gram-negative organisms and *Candida albicans*.

Each bar in figure 3. 1 represents the mean ± SD of the ZOI of each sample against MSSA and MRSA. All the data scattered within normal distribution and three groups are significant at 95% significance level (independent sample T-test: $p < 0.05$). Although sample A had an effect on both MSSA and MRSA in the same manner (p = 0.350), samples B (P = 0.010) and C (P = 0.001) had a significantly higher effect on MSSA than MRSA. Further, Figure 3.2 shows the formation of clear inhibition zones because of the three combinations of *Panchavalkala* reacting against the MSSA and MRSA.

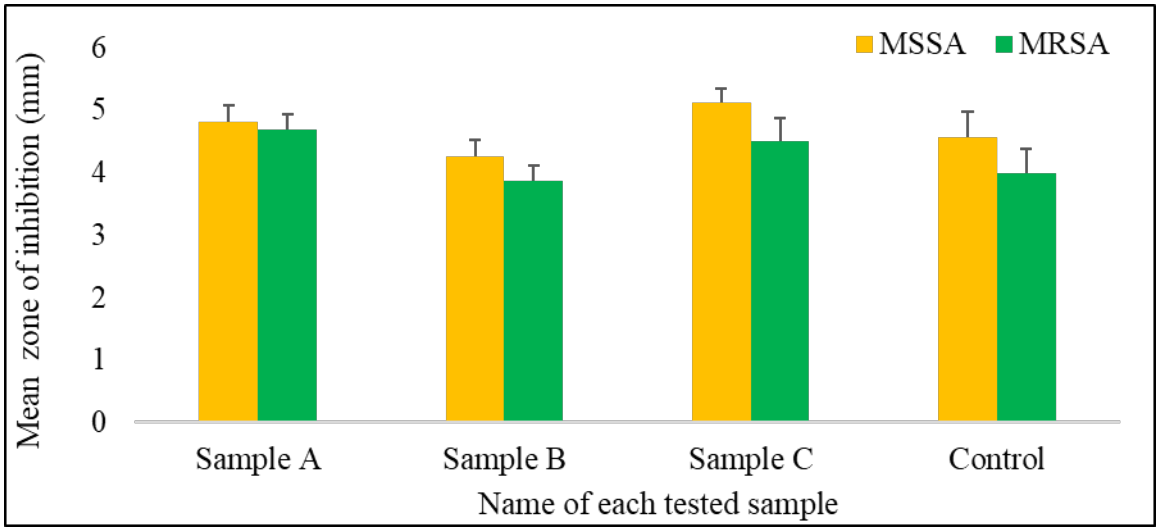

Figure 3.1: Mean ZOI of three *Panchavalkala* combinations and positive controls against MRSA and MSSA.

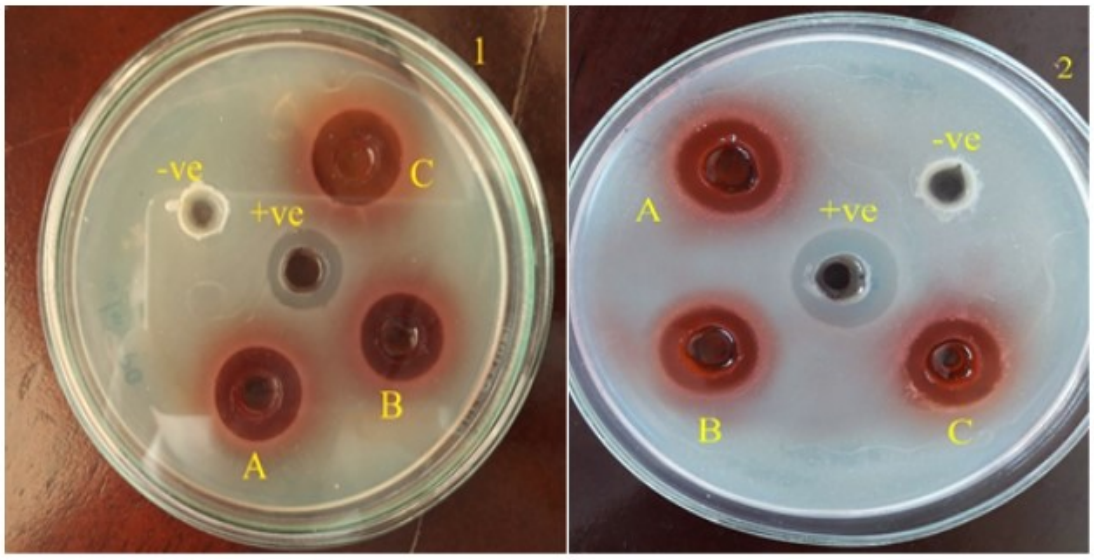

Figure 3.2: Antimicrobial activity of each *Panchavalkala* sample (A, B, C,) with positive (+Ve) and negative (- Ve) controls against 1. MSSA and 2. MRSA.

3.1.2 Antimicrobial activity of *Panchavalkala* against clinical isolates

For further confirmation of antimicrobial activity of Panchavalkala against Gram positives (MSSA and MRSA), all three combinations were tested against clinical isolates of both MSSA and MRSA.

Table 3.2: Mean zone of inhibition (ZOI) of each *Panchavalkala* combination and range of the ZOI against clinically isolated MSSA and MRSA.

	Microorganism and ZOI in (mm)			
Sample	*S. aureus*	Range	MRSA	Range
A	2.85 ± 0.36	(2.50 - 3.75)	2.82 ± 0.51	(2.00- 3.50)
B	2.55 ± 0.30	(1.75 - 2.75)	2.42 ± 0.50	(1.75 - 3.50)
C	2.92 ± 0.41	(2.50 - 3.75)	2.80 ± 0.52	(2.25 - 3.75)
Amoxicillin	5.95 ± 1.14	(5.00 - 7.75)		
Vancomycin			4.20 ± 0.33	(2.75 - 6.75)

The above table illustrates the mean ± SD of ZOI of *Panchavalkala* samples A, B, and C against ten clinical isolates of MSSA and MRSA. Both groups were significantly inhibited by *Panchavalkala* at a 95% significance level. (Independent sample T-test: $p < 0.05$). Zones of inhibition of samples A, B, and C against clinical isolates of MSSA and MRSA were 2.85 ± 0.36 mm and 2.82 ± 0.51 mm, 2.55 ± 0.30 mm and 2.42 ± 0.50, 2.92 ± 0.41 mm and 2.80 ± 0.52 mm respectively.

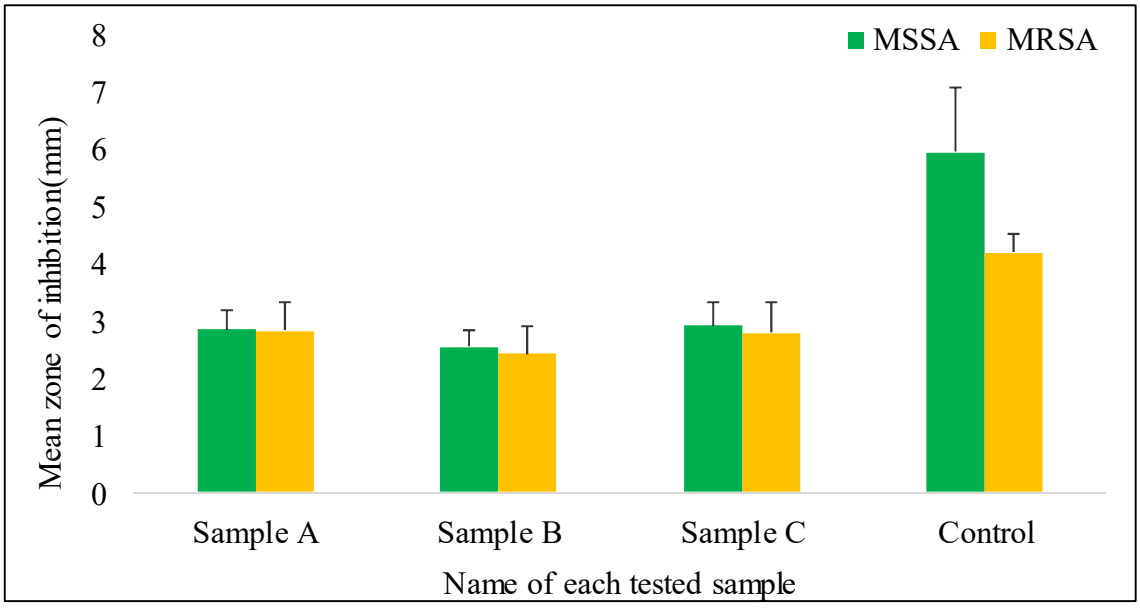

Figure 3.3: Mean ZOI of three *Panchavalkala* combinations and positive controls against clinical isolations of MSSA and MRSA.

Each of the three samples had given ZOI against tested clinical isolates but they were not significantly different from each other. However, control samples have shown a significantly high inhibition when compared to all three *Panchavalkala* samples (P = 0.000). Figure 3.3 gives a clear idea about the results.

3.1.3 Antimicrobial activity of individual plants used for *Panchavalkala*

Following the above result antimicrobial properties of individual plant barks were studied to identify whether they have an antimicrobial activity when they are used alone. Antimicrobial effects of all plant bark were tested against standard isolations of bacteria.

The table 3.3 and figure 3.4 illustrates the mean ± SD of ZOI of each plant containing *Panchavalkala* samples A, B, and C against tested wound pathogens. All plant bark extracts did not show any inhibition against *E. coli*, *Pseudomonas* and *Candida.* But all plant extracts except *A. indicum* showed antimicrobial effects against MRSA and MSSA. However, *F. benghalensis, F. racemose, C. cainito* have similarly effect as amoxicillin against MSSA while the *F. religiosa, F. arnottiana, T. populnea, and G. quesita have* not shown a significant effect. All the plant extracts have no significant effect ($p > 0.05$) on MRSA when compared to vancomycin. Appendix 2 shows the ZOI of each plant extract against MRSA and MSSA.

Table 3.3: Mean Zone of Inhibition (ZOI) of each plant bark containing three *Panchavalkala* combinations against standard isolations of wound pathogens.

	Microorganism and ZOI in (mm)				
Sample	*E. coli*	*Pseudo*	*Candida*	MRSA	MSSA
F. bengalensis	No ZOI	No ZOI	No ZOI	3.81 ± 0.59	4.68 ± 0.26
F. racemose	No ZOI	No ZOI	No ZOI	3.94 ± 0.62	4.50 ± 0.38
F. religiosa	No ZOI	No ZOI	No ZOI	2.88 ± 0.79	3.75 ± 0.46
F. arnotiana	No ZOI	No ZOI	No ZOI	3.56 ± 0.32	3.94 ± 0.32
G. quesita	No ZOI	No ZOI	No ZOI	3.31 ± 0.37	3.68 ± 0.53
T. populnea	No ZOI	No ZOI	No ZOI	3.31 ± 0.37	3.06 ± 0.50
A. indicum	No ZOI	No ZOI	No ZOI	No ZOI	No ZOI
C. cainito	No ZOI	No ZOI	No ZOI	4.50 ± 0.37	4.44 ± 0.32
Control	5.21 ± 0.39	3.07 ± 0.78	3.07 ± 0.53	5.14 ± 0.30	4.82 ± 0.54

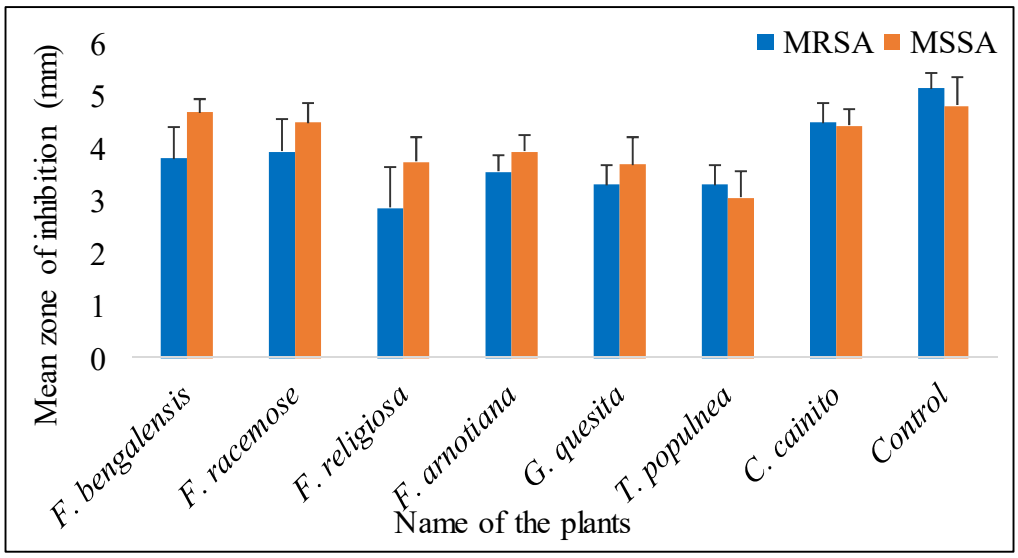

Figure 3.4: Mean ZOI of each water extraction of plant barks against MSSA and MRSA.

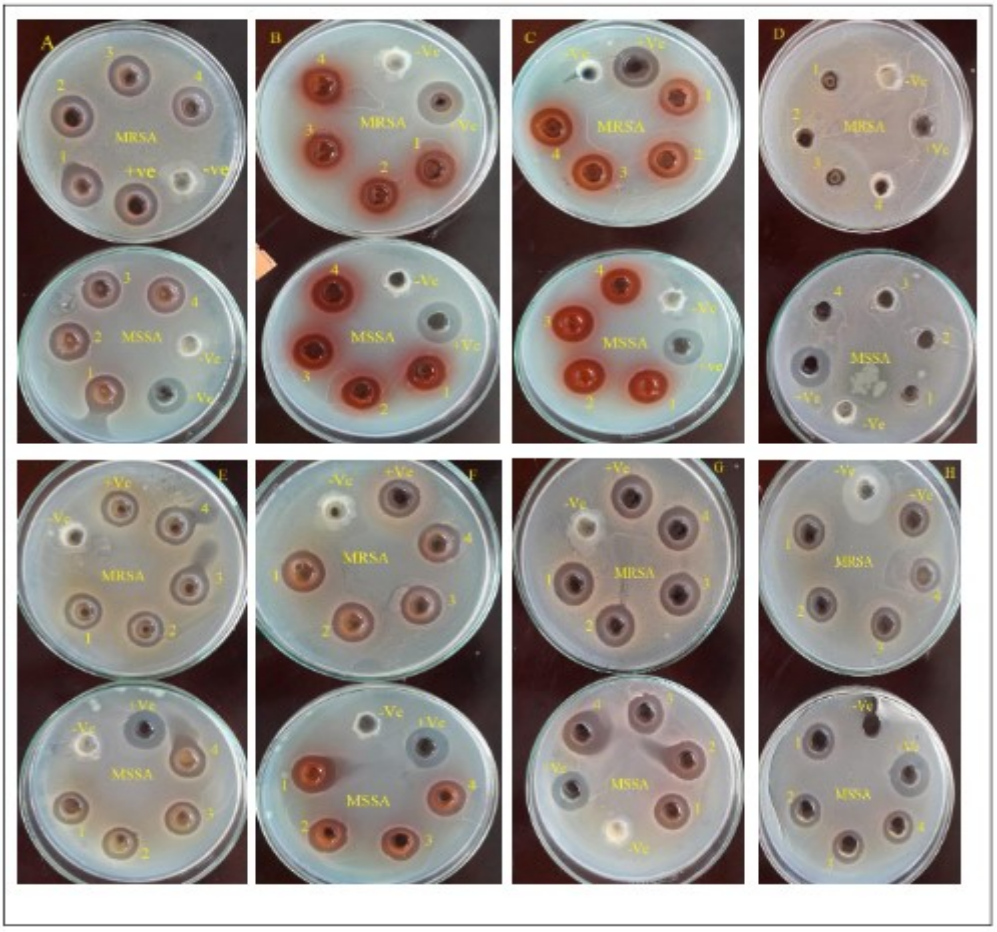

Figure 3.5: Zone of inhibition given by each plant extract against MSSA and MRSA *in vitro* study.

A. ZOI of *F. racemosa* bark extract against MRSA and MSSA.
B. ZOI of *F. religinosa* bark extract against MRSA and MSSA.
C. ZOI of *F. bengalensis* bark extract against MRSA and MSSA.
D. ZOI of *A. indicum* bark extract against MRSA and MSSA.
E. ZOI of *G. quaesita* bark extract against MRSA and MSSA.
F. ZOI of *F. arnottiana* bark extract against MRSA and MSSA.
G. ZOI of *C. cainito bark* extract against MRSA and MSSA.
H. ZOI of *T. populnea* bark extract against MRSA and MSSA

Vancomycin used as +Ve control for MRSA while Amoxicillin for MSSA. SD water used as a -Ve control.

3.2 Characterization of silver nanoparticles synthesized from *Panchavalkala*

3.2.1 Visual observation and physiochemical characterizations

Table 3.4: Color and pH changes of each plant extraction before and after the formation of silver nanoparticles.

Plant extract + $AgNO_3$	Color changes		pH changes (25 °C)	
	Initial	After	Initial	After
A	Light yellow	Reddish-brown	4.98	5.60
B	Dark yellow	Reddish-brown	5.44	5.60
C	Light yellow	Reddish-brown	5.23	5.34
$AgNO_3$ + PVA	Colorless	Brownish-yellow	6.50	8.00

The reduction of Ag^+ to Ag^0 was confirmed by the color changes of the samples from yellow to reddish-brown and finally to colloidal brown due to the excitation of surface plasmon vibrations in Ag-NPs. The initial pH of samples A, B, and C at 25 °C respectively were 4.98, 5.44, and 5.23. In the end, they were increased up to 5.60, 5.60, and 5.34 respectively (Table 3.4). The color change of each sample was observed. While the initial color of samples A and C were light yellow, sample B appeared to be a bit dark (Figure 3.6). The color of each sample was converted to reddish-brown (Figure 3.7) within a maximum period of 20 minutes confirming the formation of silver nanoparticles. Initial sample that containing $AgNO_3$ + PVA was colorless and after one hour heating process the color changed to brownish yellow.

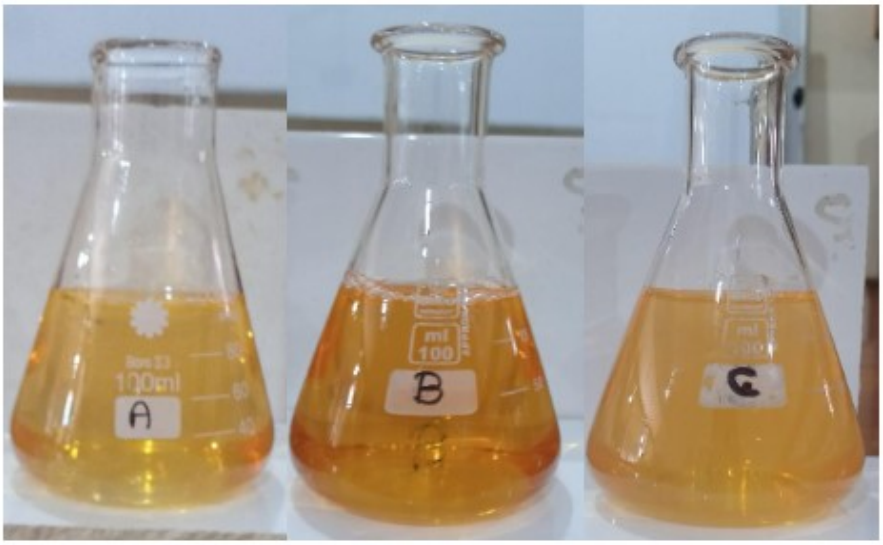

Figure 3.6: Initial texture of each water extraction of *Panchavalkala* (A, B, C) after adding 1mM silver nitrate

Figure 3.7: Digital optical images of the three samples of *Panchavalkala* after synthesis of silver nanoparticles.

3.2.2 Ultraviolet-visible spectroscopy analysis

UV-vis spectroscopy is an extremely useful and reliable technique for the primary characterization of synthesized nanoparticles as it is a fast, easy, simple, sensitive, and selective method for the identification of different types of NPs. It needs only a short period for measurement, and finally, calibration is not required for particle characterization of colloidal suspensions. UV-vis spectroscopy is also used to monitor the synthesis and stability of Ag-NPs. They have unique optical properties which make them strongly interact with specific wavelengths of light. In Ag-NPs, the conduction band and valence band lie very close to each other thus enabling free movement of the electrons. These free electrons give rise to a Surface Plasmon Resonance (SPR) absorption band, occurring due to the collective oscillation of electrons of silver nanoparticles in resonance with the light wave. The absorption of Ag-NPs depends on the size of the particles, dielectric medium, and chemical surroundings. Observation of this peak assigned to a surface plasmon is well documented for various metal nanoparticles with sizes ranging from 2 to 100 nm (Zhang *et al*., 2016).

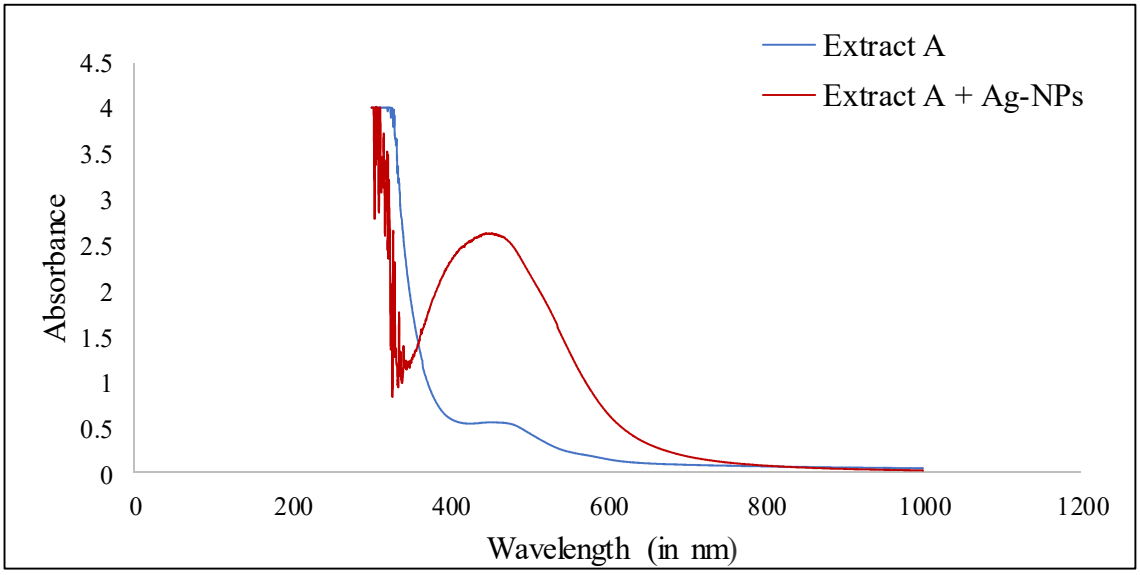

Figure 3.8: UV-vis absorption spectrum of silver nanoparticles containing *Panchavalkala* extract - A and *Panchavalkala* extract – A (without silver nanoparticles).

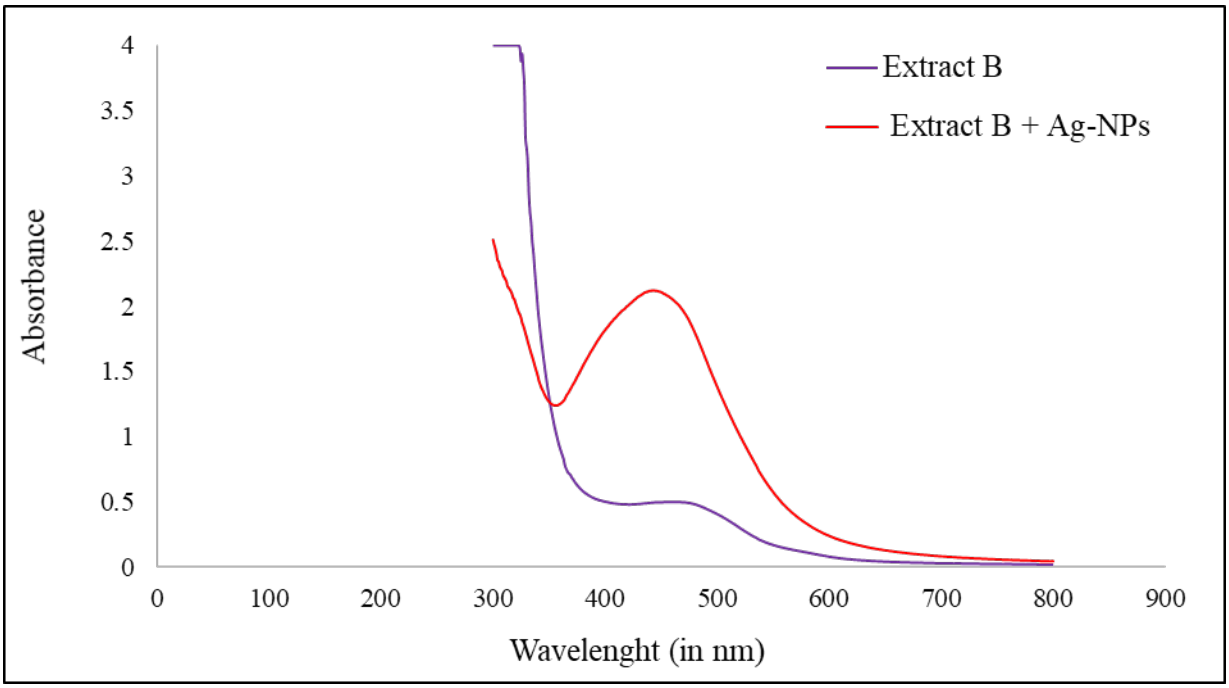

Figure 3.9: UV-vis absorption spectrum of silver nanoparticles containing *Panchavalkala* extract - B and *Panchavalkala* extract – B (without silver nanoparticles).

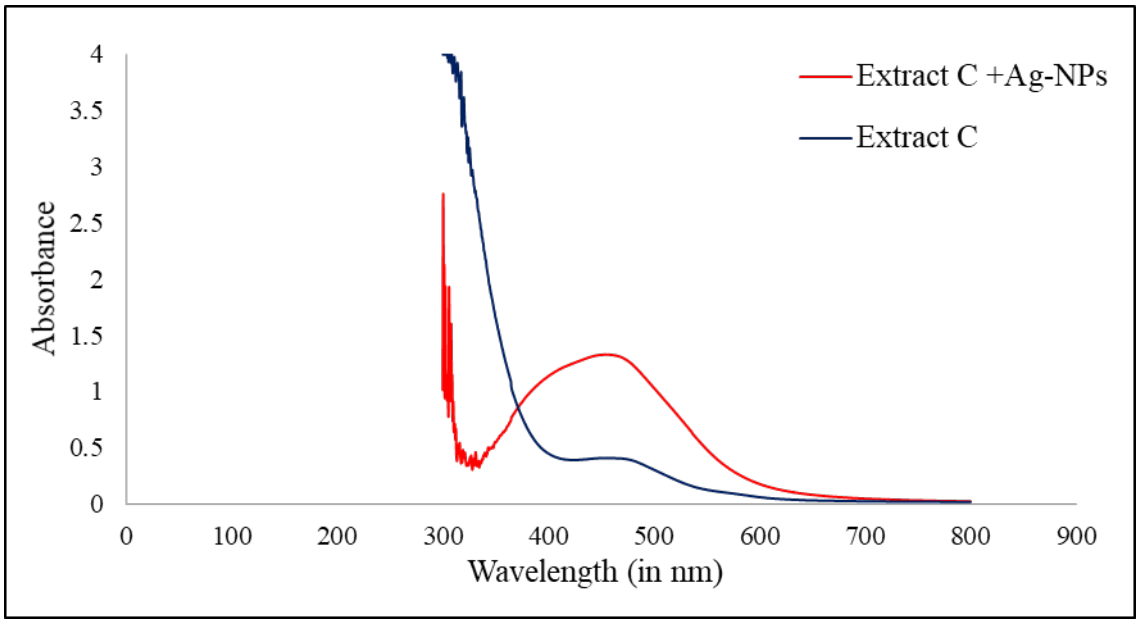

Figure 3.10: UV-vis absorption spectrum of silver nanoparticles containing Panchavalkala extract - C and Panchavalkala extract – C (without silver nanoparticles).

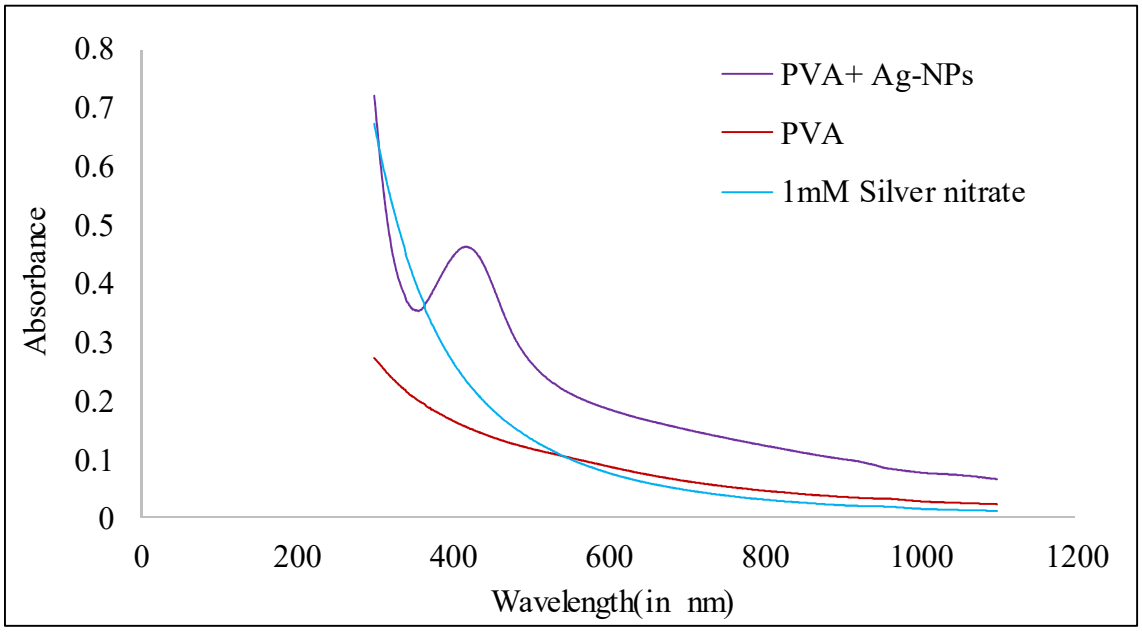

Figure 3.11: UV-vis absorption spectrum of silver nanoparticles containing PVA solution, 5% PVA solution (without silver nanoparticles) and 1mM silver nitrate solution

According to Sastry *et al*., Ag- NPs have demonstrated a peak centered within the range of 400 – 450 nm due to the SPR. Thus, it is the significant range of Ag-NPs at UV-vis spectra and corresponds to the absorbance of Ag-NPs (Sastry *et al*., 1997). In this study, the UV-vis spectra of silver nanoparticles synthesized using *Panchavalkala* extract - A displayed a strong broad peak around 444 nm due to the formation of Ag- NPs (figure 3.8). Further, Ag -NPs synthesized using *Panchavalkala* extracts B and C also displayed broad peaks respectively around 445 nm (figure 3.9) and 444.5 nm (figure 3.10). Thus, Ag -NPs synthesized using PVA displayed broad peaks around 420nm (figure 3.11).

3.2.3 Scanning Electron Microscopy (SEM) analysis

Recently, the fields of nanoscience and nanotechnology have provided a driving force in the development of various high-resolution microscopy techniques to learn more about nanomaterial using a beam of highly energetic Electrons to probe objects on a very fine scale. Among various electron microscopy techniques, SEM is a surface imaging method that is fully capable of resolving different particle sizes, size distributions, nanomaterial shapes, and the surface morphology of the synthesized particles at the micro and Nano scales. Using SEM, the morphology of particles can be probed to derive a histogram from the images either by measuring and counting the particles manually or by using specific software. Although SEM can provide valuable information regarding the purity and the degree of particle aggregation, its inability to resolve the internal structure of the particles is highlighted as a downside (Zhang *et al*., 2016).

SEM technique was employed to determine the surface morphology and the topography of synthesized silver nanoparticles. Figure 3.12 shows the size of silver nanoparticles that were synthesized from the Panchavalkala combination - A with an average size of 79.94 nm. The average size of silver nanoparticles that were synthesized from Panchavalkala combinations B (Figure 3.13) and C (Figure 3.14) was 112.76 nm and 88.19 nm respectively. These SEM images showed that the green synthesized silver nanoparticles were mostly spherical. Figure 3.15 shows SEM image of silver nanoparticles, chemically synthesized by reaction of 1mM silver nitrate and 5% PVA.

The SEM image analysis demonstrates that the synthesis of the Ag-NPs was due to the interaction of the hydrogen bond and the electrostatic interaction between the bio-organic capping molecules bound to Ag-NPs. The NPs were not in direct contact even within the aggregates, indicating stabilization of the NPs by a capping agent. The large Ag-NPs may occur due to the aggregation of smaller ones.

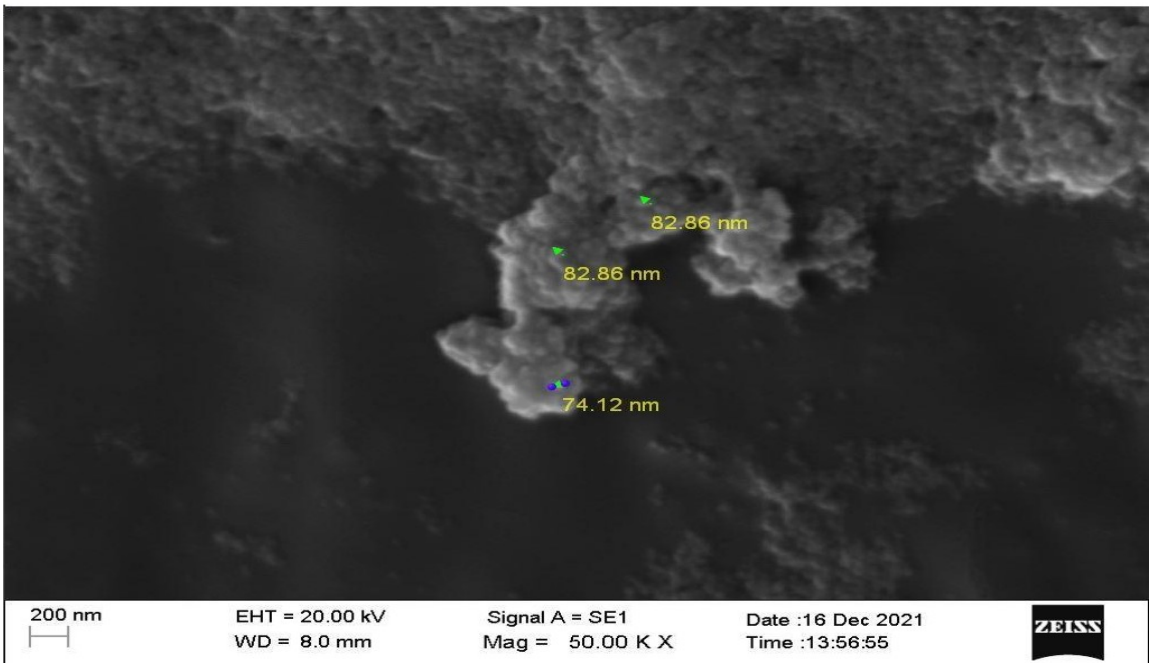

Figure 3.12: SEM image of silver nanoparticles formed by the reaction of 1mM silver nitrate and the extract of *Panchavalkala* combination - A.

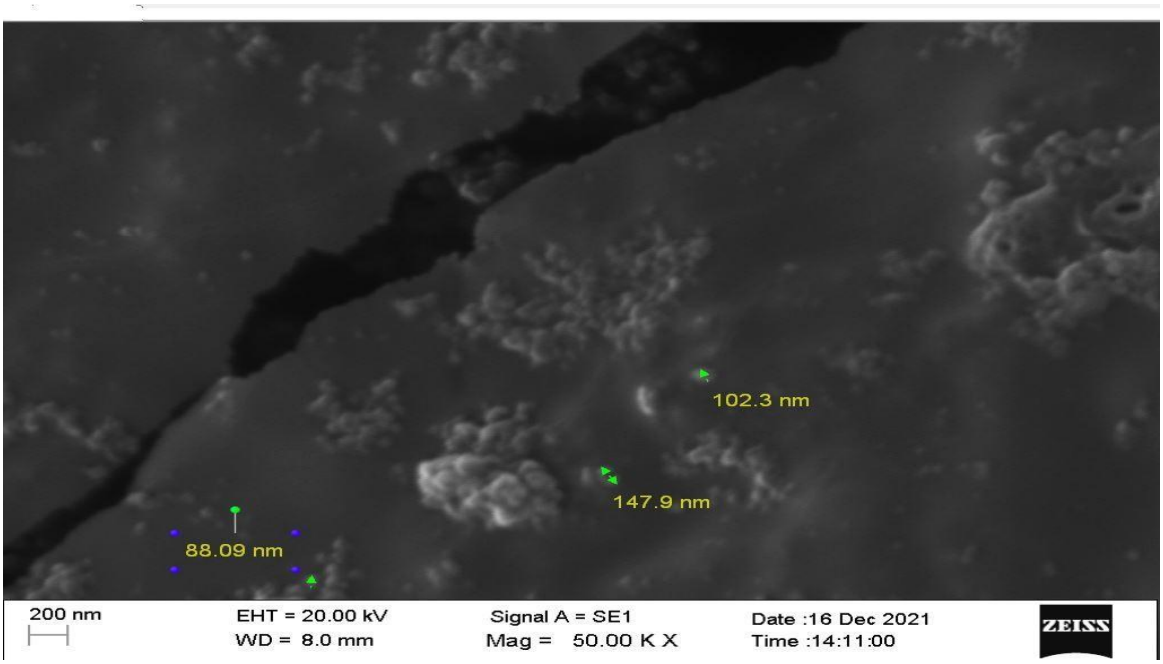

Figure 3.13: SEM image of silver nanoparticles formed by the reaction of 1mM silver nitrate and extract of *Panchavalkala* combination B.

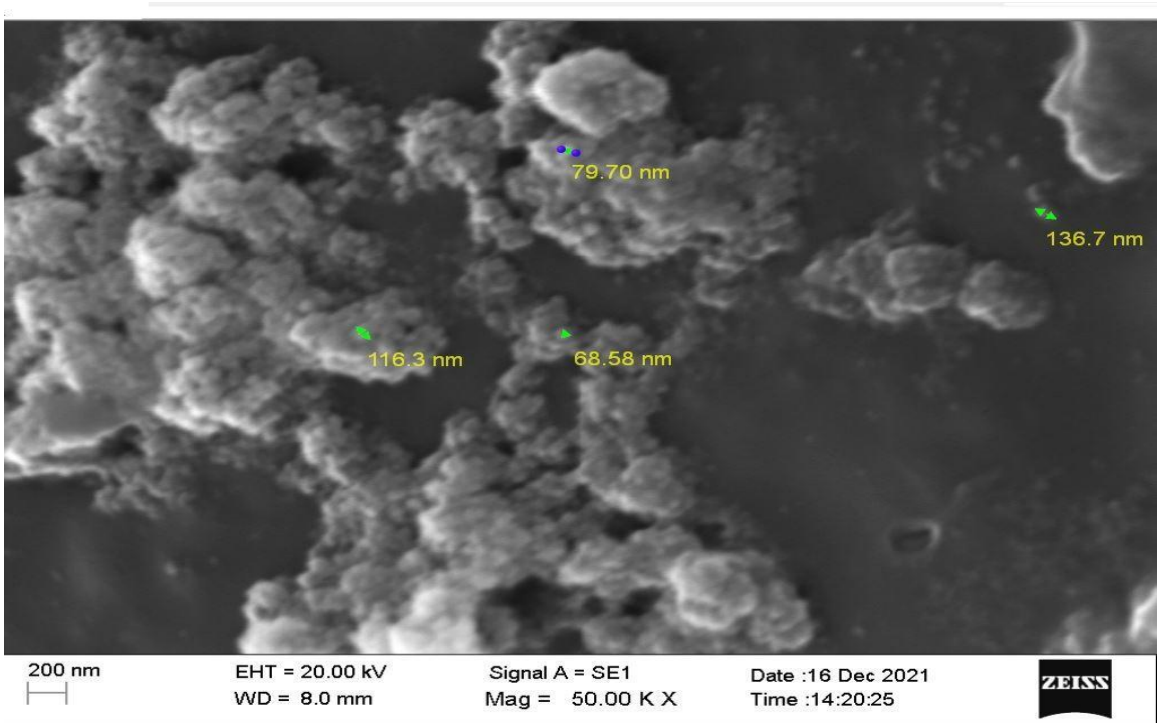

Figure 3.14: SEM image of silver nanoparticles formed by the reaction of 1mM silver nitrate and extract of *Panchavalkala* combination C.

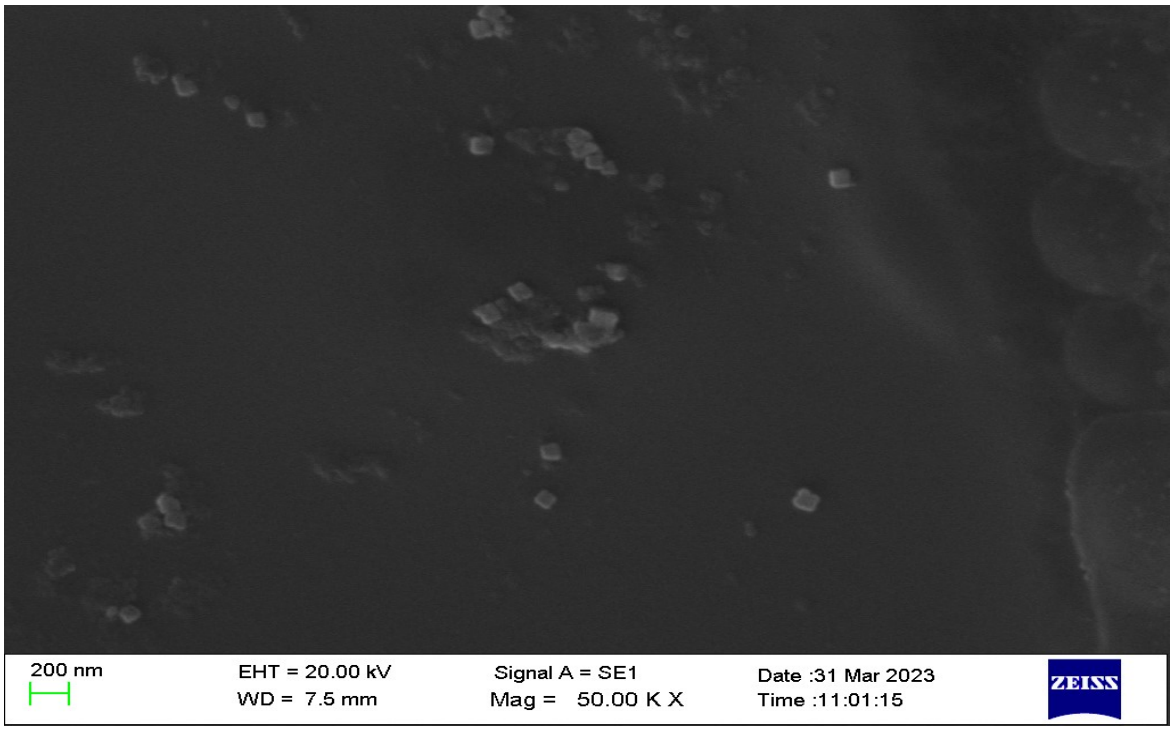

Figure 3.15: SEM image of silver nanoparticles, chemically synthesized by the reaction of 1mM silver nitrate and5% PVA.

3.3 Analysis of Antimicrobial property of silver nanoparticles

3.3.1 Antimicrobial activity of Ag-NPs against standard isolates of common wound pathogens

Table 3.5: Mean Zones of Inhibitions (ZOI) of silver nanoparticles synthesized from each *Panchavalkala* extraction, 1mM silver nitrate aqua solution and positive controls against standard common pathogens that cause wound infections. (A- Ag-NPs; sample A that contains silver nanoparticles, B- Ag-NPs; sample B that contains silver nanoparticles, C- Ag-NPs; sample C that contains silver nanoparticles).

	Microorganism and ZOI in (mm)				
Sample	*E. coli*	*Pseudomonas*	*S. aureus*	MRSA	*Candida*
A- Ag-NPs	1.94 ± 0.49	2.62 ± 0.35	2.00 ± 0.46	2.31 ± 0.26	2.19 ± 0.84
B- Ag-NPs	2.18 ± 0.53	2.75 ± 0.37	2.62 ± 0.23	3.00 ± 0.38	2.94 ± 0.32
C- Ag-NPs	2.37 ± 0.79	2.94 ± 0.32	2.19 ± 0.26	2.94 ± 0.32	3.56 ± 0.32
Gentamycin	6.12 ± 1.70	2.69 ± 0.26			
Amoxicillin			4.97 ± 0.32		
Vancomycin				4.56 ± 0.32	
Silver nitrate	2.00 ± 0.26	2.44 ± 0.32	0.51 ± 0.03	2.88 ± 0.32	4.06 ± 0.32
fluconazole					5.00 ± 0.38

In this study, the antimicrobial property of Ag-NPs was evident against the *E. coli*, *Pseudomonas aeruginosa*, *S. aureus*, methicillin-resistant *S. aureus,* and *Candida*. The results obtained are shown in Table 3.5. The inhibition zones obtained indicate maximum antibacterial activity of each of the prepared extractions of *Panchavalkala*. All samples showed antimicrobial properties against tested microorganisms.

All three samples have given ZOI against tested microorganisms. However, when compared with their positive control, the antimicrobial property of Ag-NPs synthesized from *Panchavalkala* combinations A, B, and C have not shown significant difference in inhibition of *E. coli*, *Pseudomonas*, *Candida*, *S. aureus* and methicillin-resistant *S. aureus* ($p > 0.05$).

Figure 3.16 shows the mean ZOI and standard deviations (SD) of synthesized silver nanoparticles from three *Panchavalkala* combinations, positive controls, and 1mM silver nitrate solution against tested standard wound pathogens.

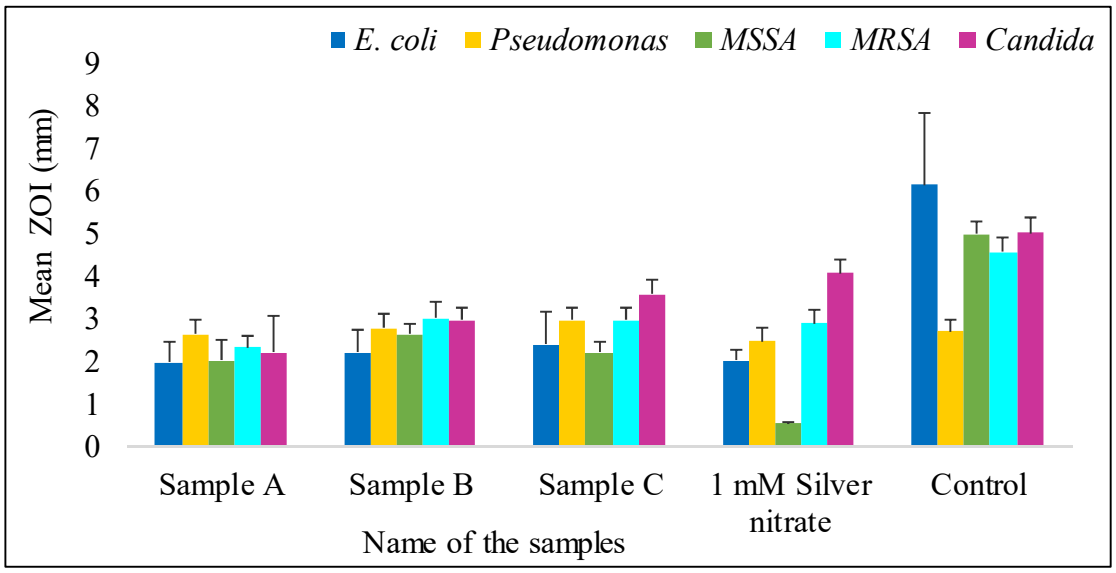

Figure 3.16: Mean ZOI of synthesized silver nanoparticles from three *Panchavalkala* combinations, positive controls (Gentamycin for *E. coli* and *Pseudomonas*, Amoxicillin for MSSA, Vancomycin for MRSA, Fluconazole for *Candida*) and 1mM silver nitrate solution against tested wound pathogens.

However, there was no significant difference in the ZOI gained by the three *Panchavalkala* samples which contained Ag-NPs and silver nitrate against *E. coli* ($p > 0.05$). There was a similar effect of Ag- NPs synthesized from *Panchavalkala* extract A, B and silver nitrate against *Pseudomonas* while Sample C had a significant effect than silver nitrate ($P = 0.008$). All three samples had significant effects on MSSA than silver nitrate ($P = 0.000$). Thus, silver nitrate showed significant inhibition ($P = 0.016$) against MRSA than Ag-NPs synthesized from sample A while it showed similar effect as samples B and C ($p > 0.05$). Silver nitrate showed significant effects on *Candida albicans* than other three *Panchavalkala* samples which contained Ag-NPs ($p < 0.05$).

There were no Ag- NPs containing samples that showed significant inhibition zones against *E. coli* and *Pseudomonas*. Synthesized Ag- NPs from Panchavalkala extract B had significant effects on MSSA ($p < 0.05$) when compared to other two samples A and C. Ag- NPs containing Sample B and C showed significantly higher effect ($p < 0.05$) on MRSA as well as *Candida albicans* than sample A.

Furthermore, figure 3.17 demonstrates the antimicrobial effects of Ag-NPs synthesized from the three combinations of *Panchavalkala*.

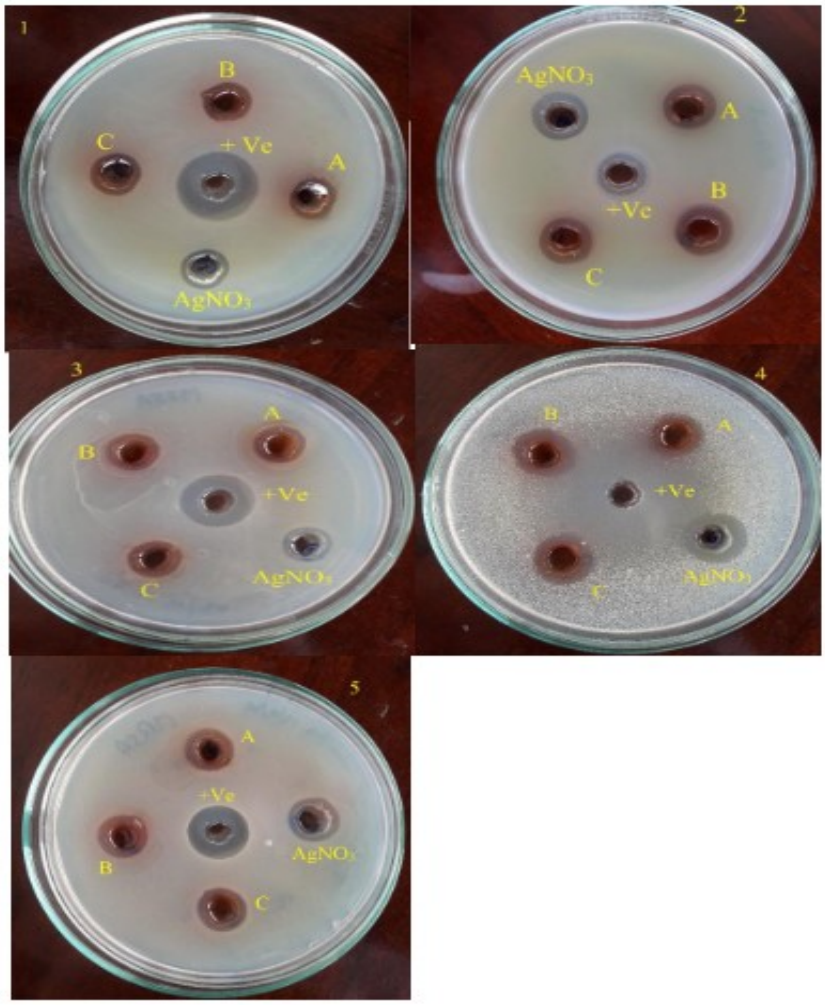

Figure 3.17: Antimicrobial activity of each *Panchavalkala* sample A, B, C, with positive and 1mM silver nitrate against 1. *E. coli*, 2. *Pseudomonas*,3. MSSA, 4. *Candida albicans* 5. MRSA.

All three samples that contained Ag-NPs showed antimicrobial effects against tested microorganisms; however, antimicrobial activity of all three samples against MSSA and MRSA have reduced when compared to the *Panchavalkala* samples without containing Ag-NPs. This may happen due to the reaction of phytochemicals contained in bark extract of the herbs and may be used in the formation of capping agents. Therefore, the number of phytochemicals that have antimicrobial effects may be reduced after the formation of Ag-NPs. This result needs further investigations in future experiments.

Table 3.6: Mean Zones of Inhibitions (ZOI) of each extract of *Panchavalkala* (without Ag-NPs) and silver nanoparticles containing Panchavalkala (with Ag-NPs), against MSSA and MRSA.

	Microorganism and ZOI in (mm)			
Organism	MSSA		MRSA	
Sample	Without NPs	With NPs	Without NPs	With NPs
A	4.81 ± 0.26	2.00 ± 0.46	4.69 ± 0.26	2.31 ± 0.26
B	4.25 ± 0.27	2.62 ± 0.23	3.88 ± 0.23	3.00 ± 0.38
C	5.12 ± 0.23	2.19 ± 0.26	4.50 ± 0.38	2.94 ± 0.32

The above table 3.6 illustrates the mean ± SD of ZOI without silver nanoparticles and with silver nanoparticles from *Panchavalkala* samples A, B, and C against MSSA and MRSA. Both groups are significant at a 95% significance level.

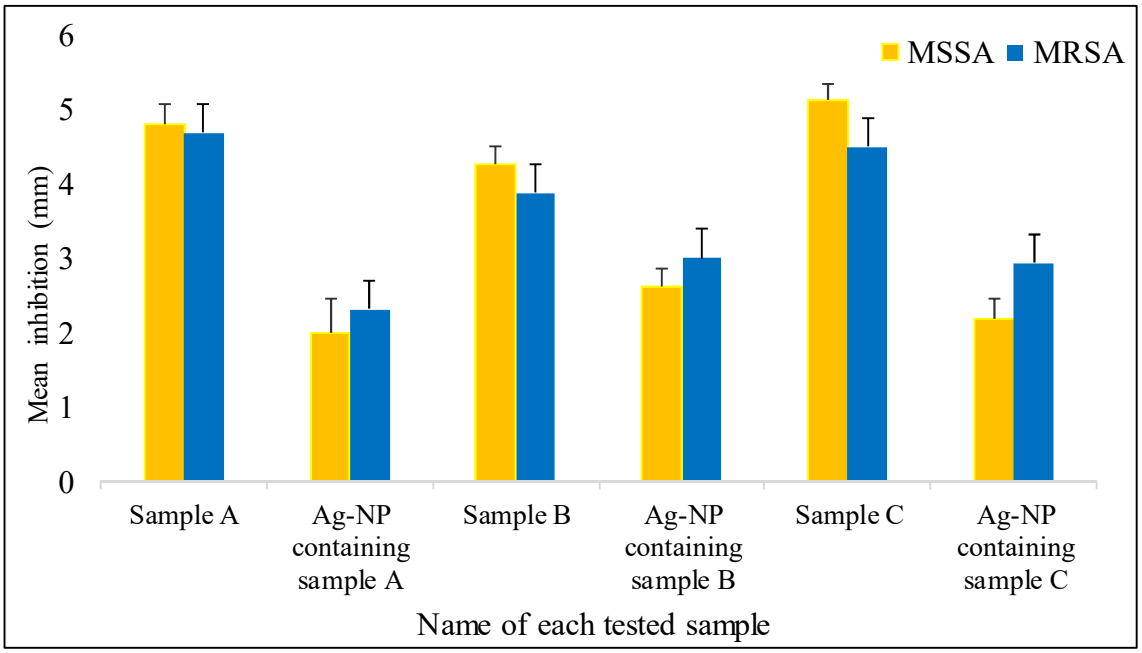

Figure 3.18: Mean ZOI differences of samples A, B, and C before and after the synthesis of Ag-NPs against MSSA and MRSA.

Each bar in figure 3.18 represents the Mean ± SD of the ZOI of each sample before and after the synthesis of Ag- NPs against MSSA and MRSA. All the data were scattered within normal distribution. All groups are significant at a 95% significance level (Paired sample T-test: $p < 0.05$).

Panchavalkala sample B significantly inhibited (P = 0.010) MSSA than MRSA. Similarly, Ag-NPs, synthesized from sample B significantly inhibited (P = 0.035) MRSA than MSSA. Sample A (P = 0.350) and nanoparticles synthesized from sample A (P = 0.118) had no significant effect on both microorganisms. Sample C showed significant effects (P = 0.001) on MSSA than MRSA and after synthesis of Ag-NPs, it had significant inhibitory effect (P = 0.000) on MRSA than MSSA.

3.3.2 Antimicrobial activity of Ag-NPs against clinical isolates

Furthermore, Antimicrobial activity of Ag-NPs against MSSA and MRSA were studied using clinical isolates of MSSA and MRSA (table 3.7) to identify whether there are significant differences between standard and clinical isolates. However, according to the result there were no significant differences in the effect between standard and clinical isolates. Therefore, it is likely that both *Panchavalkala* and its Ag-NPs act against MSSA and MRSA irrespective of their origin; standard or clinical isolates in a similar manner.

Table 3.7: Mean zone of inhibition (ZOI) of each Ag-NPs and range of the ZOI against clinically isolated MSSA and MRSA.

	Microorganism and ZOI in (mm)			
Sample	*S. aureus*	Range	MRSA	Range
A	2.50 ± 0.32	(2.00 -2.75)	2.60 ± 0.25	(1.50 -3.00)
B	2.83 ± 0.38	(2.00- 3.50)	3.25 ± 0.42	(2.50- 3.75)
C	2.25 ± 0.26	(1.25- 3.75)	2.95 ± 0.35	(2.50 -3.50)
Amoxicillin	4.50 ± 0.39	(5.00-7.50)		
Vancomycin			4.83 ± 0.36	(3.00 -5.75)

Above table 3.7 illustrates the mean ± SD of ZOI of Ag-NPs synthesized from *Panchavalkala* samples A, B, and C against ten clinical isolates of MSSA and MRSA. Both groups have significantly inhibited at a 95% significance level. (Independent sample T-test: $p < 0.05$). Zones of inhibition of samples A, B, and C against clinical isolates of MSSA and MRSA were 2.50 ± 0.32 mm and 2.6. ± 0.25 mm, 2.83 ± 0.38 mm and 3.25 ± 0.42, 2.25 ± 0.26 mm and 2.75± 0.95 mm respectively.

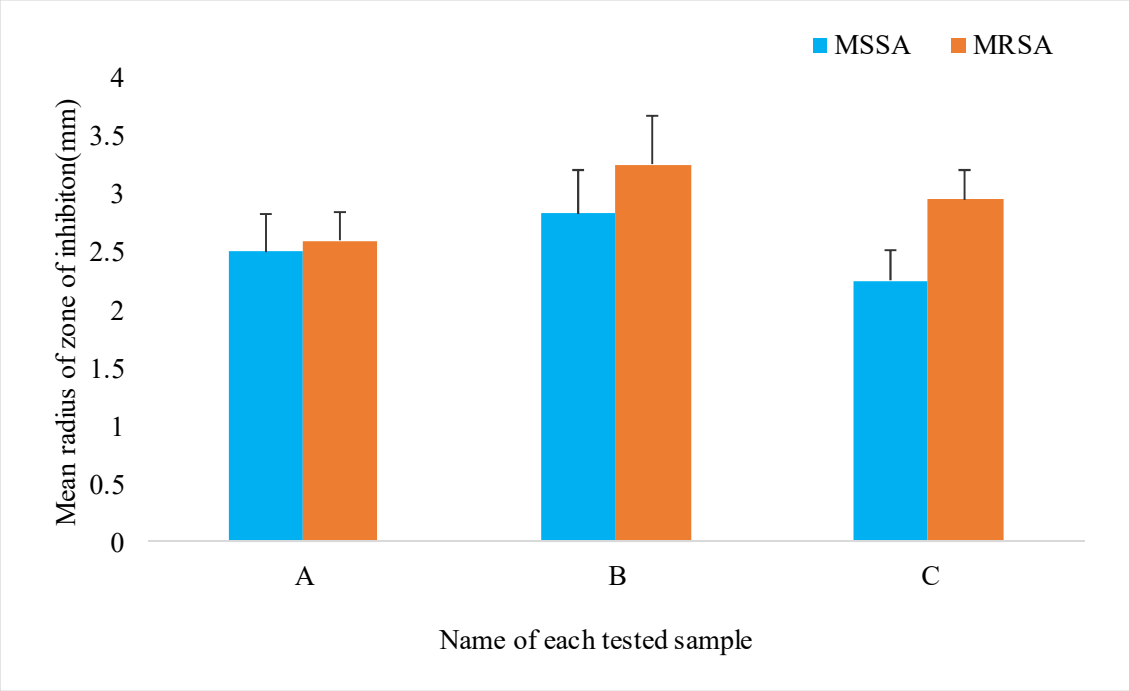

Figure 3.19: Mean ZOI of Ag-NPs synthesized from each Panchavalkala combination against clinical isolation of MSSA and MRSA.

Each bar in figure 3.19 represents the Mean ± SD of the ZOI of each sample of Ag- NPs against MSSA and MRSA. All the data were scattered within normal distribution. All groups are significant at a 95% significance level (Paired sample T-test: $p < 0.05$). Sample B (P = 0.000), as well as C (P = 0.000) significantly inhibited MRSA and MSSA, but sample A had no significant effect on both microorganisms.

Veerasamy *et al*., have demonstrated that the pH of the medium of the solution was an important

factor that influences both rate, shape and size of plant-mediated biosynthesized Ag-NPs. The presence of large numbers of functional groups at higher pH, leads to nucleation at that higher pH while at lower pH aggregation was favored over nucleation thus confirming that nucleation increases with increasing pH of the solution proving the formation of Ag^0 from Ag^+ due to bioreduction. They also showed that pH of the solution additionally influences the rate of bioreduction by influencing the activity of phytochemicals (Veerasamy *et al*., 2011). Better Ag-NPs formation occurred under basic conditions with 0.1-2.0 $AgNO_3$ and efficiency decreased with decreasing pH of the reaction medium (Yazdi et al., 2019). Furthermore, Khandan *et al*., observed that yielded larger size of Ag-NPs synthesized in acidic medium (pH = 4) whereas highly dispersed and small sized Ag-NPs synthesized at pH 8 (Khandan *et al*., 2020).

The preparations of *Panchavalkala* A, B and C used in this study also create a medium with acidic pH values of 5.6, 5.6, and 5.34 (Table 3.4) respectively. The synthesized nanoparticles from each sample showed higher aggregation with increase of size of nanoparticles.

Uv-vis spectroscopy is an indirect method to examine the bio-reduction of Ag-NPs from aqueous $AgNO_3$ solution. Synthesis of metallic Ag-NPs was further confirmed with Uv-vis characteristic absorption band of silver nanoparticles (Shameli *et al*., 2012). According to Mie's theory spherical metal nanoparticles can only give a single surface plasmon resonance (SPR) band while anisotropic particles could give two or more than two SPR bands depending upon the shape of nanoparticles (He *et al*., 2002). Since, in this present study a single SPR band was observed going by Mie's theory synthesized silver nanoparticles were spherical in shape.

According to Sastry, Ag-NPs have demonstrated a peak centered within the range of 400-450 nm due to the SPR (Sastry *et al*., 1997). In this present study also Ag-NPs containing sample A, B and C respectively displayed a strong band peak around 444 nm, 445nm and 444.5 nm thus confirming the formation of silver nanoparticles.

According to Shaikh *et al*., carbonyl and hydroxyl groups of flavonoids play a significant role in the reduction of Ag^+ through the metal chelation with the catechol moiety of flavonoids, where the electrostatic interaction and charge transfer between the OH group of flavonoids and Ag^+ are responsible for biochemical interaction to bio reduction (Shaikh *et al*., 2020). All the plant materials used in this study are rich in flavonoids. As such these plant materials can confidently be said to promote reduction of Ag^+. In addition to this benefit from the plant extracts used in this study, the use of a combination of different plant extracts is highly beneficial as they act synergistically in the bioreduction of Ag^+ as suggested by Liaqat *et al*., who concluded that instead of a single plant extract, plants in combination synthesized nanoparticles in a shorter time with better characteristics. In combinations the bioactive components certainly imparted a synergistic effect for bioreduction of Ag^+ into Ag^0 nanoparticles (Liaqat *et al*., 2022). The multi resistant pathogens due to antigenic shift and drifts are ineffectively managed with modern medications. This is a serious problem in public health. Therefore, there is a necessity to develop novel antimicrobial agents. Silver ions have a long history of use as an antiseptic and disinfectant and are able to interact with disulphide bonds of glycoprotein contents of microorganisms and change the three-dimensional structure. This property can be used to block the functional operations of the microorganism

(Shakeel *et al*., 2016). Advancement of this green synthesis over chemical and physical methods is that it is cost effective, environment friendly, easily scaled up for large scale synthesis and there is no need of using high energy, pressure, temperature and toxic chemicals (Zhang *et al*., 2010). These advantages opened the doors to explore benign and green routes for synthesizing nanoparticles.

The present study showed the antimicrobial property of alternative three *Panchavalkala* combinations used in Sri Lanka. Mainly all three combinations gave an antimicrobial effect against both MSSA and MRSA. In Particular, combination C had a higher effect on MSSA (P = 0.005) when compared to the control and other two combinations. Combinations A (P =0.001) and C (P = 0.019) had significant effect on MRSA compared to the control and the combination B. Further study of using clinical isolates of MSSA and MRSA showed that all three combinations had effect on both MRSA and MSSA but their activity were not comparable with the positive controls. Individual plant species used in *Panchavalkala* had various antimicrobial effects on MSSA and MRSA. None of them were active against E. *coli*, *Pseudomonas* and *Candida*. But all plants showed antimicrobial properties except *A. indicum* against MSSA and MRSA. Among the studied plants *F. benghalensis*, *F. racemose*, *C. cainito* had shown a similar effect as the control ($p > 0.05$) on MSSA.

This study was able to synthesize Ag-NPs using each water extraction of *Panchavalkala.* Ultraviolet-visible spectroscopy analysis and scanning electron microscopy analysis confirmed the formation of Ag-NPs from each plant extract and identified its antimicrobial effects. Ag-NPs synthesized using three different *Panchavalkala* combinations gave antimicrobial effects against all the tested microorganisms (both Gram negative, Gram positive and fungi) and had not shown significant effect ($p > 0.05$) compared to the controls.

Although there have been research findings showing antimicrobial activities attributed to Ag^+ or Ag salts and limitations of their uses, these researches also indicate that these limitations can be overcome by the Ag-NPs (Kim *et al*., 2007). Interestingly the finding of the above researches Kim *et al,* have shown that level of antimicrobial activity of $AgNO_3$ against *E. coli* is almost similar to the antimicrobial activity of Ag- NPs. Similarly, present study also found that antimicrobial activity of Ag- NPs synthesized using in each plant extract against *E. coli* was similar to the antimicrobial activity of $AgNO_3$ against *E. coli*.

Thus, the antimicrobial activity of Ag- NPs synthesized by using natural plant extract was investigated against various pathogenic organisms including *S. aureus*, P. *aeruginosa* and *E. coli* using well diffusion method by peter *et al*. And they have observed that silver nanoparticles showed efficient antimicrobial property compared to the other silver salts (Peter *et al*., 2015). However, in this study a similar effect of Ag- NPs synthesized from plant extract A, B and silver nitrate was observed against *Pseudomonas* while Sample C had a significant effect than silver nitrate. All three samples had significant effects on MSSA compared to silver nitrate. Thus, silver nitrate showed significant inhibition against MRSA than Ag-NPs synthesized from sample A while it showed similar effect as samples B and C. Not only that, silver nitrate also showed significant effects on *Candida albicans* than other three *Panchavalkala* samples which contained Ag-NPs.

Furthermore, there were no significant inhibition zones given by Ag- NPs containing samples against *E. coli* and *Pseudomonas*. Synthesized Ag- NPs from plant extract B had significant effects on MSSA when compared to other two samples A and C. Ag- NPs containing Sample B and C showed significantly higher effect on MRSA as well as *Candida albicans* than sample A. Ag- NPs contain Sample B as well as C showed significant inhibition against clinical isolates of MRSA and MSSA, but sample A had no significant effect on both microorganisms.

However, more studies should be carried out to identify molecular level interactions such as drug antagonism, additivism, or synergy of combination of Panchavalkala and Ag-NPs. And also, clinical investigation and cell cultural studies are necessary for identification of the cell toxicity and drug retention time which are important in clinical settings.

4 - Conclusion

This study was carried out to synthesize silver nanoparticles using water extracts of three alternative combinations of *Panchavalkala* and to assess their antimicrobial effect against some common wound pathogens.

Accordingly, the following conclusions were reached. `

a. Three alternative *Panchavalkala* samples (A, B and C) produced an antimicrobial effect only on MSSA and MRSA standard isolates.
b. Sample C demonstrated a significantly higher antimicrobial effect on MSSA when compared with other two samples, A and B.
c. Samples A and C showed a significantly higher inhibitory effect against MRSA when compared with the sample B.
d. All three samples; A, B, and C did not show antimicrobial effect on *E. coli*, *Pseudomonas* and *Candida albicans*.
e. All three samples; A, B, and C showed antimicrobial effects against clinical isolates of MSSA and MRSA.
f. Water extract of *A. indicum* did not demonstrate any antimicrobial effect when tested against the above-mentioned microorganisms.
g. Water extract of other plants used in *Panchavalkala* demonstrated antimicrobial effects on MSSA and MRSA. None of the plant extracts had antimicrobial effects against *E. coli*, *Pseudomonas* and *Candida albicans*.
h. Ag- NPs can be synthesized easily, cost effectively and in an eco-friendly manner by using each of the three *Panchavalkala* combinations.
i. The Ag-NPs synthesized using *Panchavalkala* samples A, B and C showed antimicrobial effects against all the tested microorganisms including standards and clinical isolates used in the current study.
j. Synthesis of Ag-NPs using *Panchavalkala* samples A, B and C produced broader antimicrobial activity but the antimicrobial activity was less than the activity produced by the pure *Panchavalkala* samples.

Acknowledgments

I am extremely grateful to my supervisor Professor. J.A.M.S. Jayatilake, Department of Oral Medicine and Periodontology, Faculty of Dental Sciences, University of Peradeniya for his motivation, continuous encouragement and untiring guidance given to me throughout my research. Without his support this study would not be a reality.

I wish to acknowledge all the academic members and supporting staff members of the microbiology laboratory of the Faculty of Dental Sciences, University of Peradeniya, especially the technical officers Mrs. M.R.D.M. Senanayake and Mrs. S.H.K. Werasekara; the lab attendant Mr. B.W.D.M.S.B. Yatawara; for their immense support, guidance, dedication and for sharing their knowledge and experience on microbiological procedures.

I am indebted to my respective course coordinator Professor Anoma Perera; the Senior Professor at the University of Peradeniya and also Professor Deepthi Yakandawala; Head of the Board of Plant Science, of Post Graduate institute of Science at the University of Peradeniya for providing enormous guidance and assistance throughout the research.

Finally, I would like to be thankful to my parents, family members and friends who were always in my side to encourage me throughout this period.

References

1. Ahamad, I. and Beg, A.Z. (2001). Antimicrobial and phytochemical studies on 45 Indian medicinal plants against multi-drug resistant human pathogens. *J Ethnopharmacol* **74**, 113-123. PMID:11167029.
2. Ahmed, S., Shakeel, A., Babu, L.S., Saiqa, I. (2016). A review on plants extracts mediated synthesis of silver nanoparticles for antimicrobial applications; A green expertise. *Journal of advanced research* **7**, 17-28.

3. Akter, M., Sikder, M.T., Rahman, M.M., Ullah, A.K.M.A., Hossain, K.F.B., Banik, S., Hosokawa, T., Saito, T., Kurasaki, M. (2018). A systematic review on silver nanoparticles-induced cytotoxicity: Physicochemical properties and perspectives. *Journal of Advanced Research* **9**, 1-16.
4. Allafchian, A.R., Bahramian, H., Jalali, S.A.H., Ahmadvand, H. (2015). Synthesis, characterization and antibacterial effect of new magnetically core-shell nanocomposites. *J. Magn. Magn. Mater* **394**, 318-324.
5. Allafchian, A.R., Mirahmadi-Zare, S.Z., Jalali, S.A.H., Hashemi, S.S., Vahabi, M.R. (2016). Green synthesis of silver nanoparticles using phlomis leaf extract and investigation of their antibacterial activity. *j Nanostruct Chem* **6**, 129-135.
6. Alwis, M.K.S.C., Bogahawatte, L.B.A.E., Gunasekara, T.D.P.C., Jayaweera, P.M., Kumarasinghe, K.G.U.R. (2021). Green Approach to Develop Antimicrobial Fabric using *Garcinia zeylanica* and Tea Waste Extract. *Proceedings of International Forestry and Environment Symposium* **25**.
7. Anandjiwal, S., Bagul, M.S., Parabia, M., Rajani, M. (2008). Evaluation of free radical scavenging activity of and Ayurvedic formulation, Panchavalkala. *Indian Journal of Pharmaceutical Science* **70**(1), 31-35.
8. Balayssac, S., Trefi, S., Gilard, V., Malet-Martino, M., Martino, R. (2009). A useful tool for analysis of complex mixtures; application to herbal drugs or dietary supplements for erectile dysfunction. *J pharm Biomed Anal* **50**, 602-12.
9. Bapat, R.A., Chaubal, T.V., Joshi, C.P., Bapat, P.R., Hira, C., et al. (2018). An overview of application of silver nanoparticles for biomaterials in dentistry. *Materials science and Engineering C* **91**, 881-898.
10. Bhardwaj, A. and Sahu, M. (2007). Role of Panchavalkala kwatha in preoperative skin preparation.*PG dissertation IMS*, BHU, Varanasi.
11. Biel, M.A., Sievert, C., Usacheva, M., Teichert, M., Balcom, J. (2011). Antimicrobial photodynamic therapy treatment of chronic recurrent sinusitis bio films. *Int.Forum Allergy Rhinol* **1**, 329-334.
12. Chunekar, K.C. (2006). Edition, *Bhava Prakasha Nighantu*, Bhava Mishra, X Edition Chaukhambha Bharati Academy, Varansi. Vataadi Varga **15**.
13. Daniela, P., Rayna, B., Todor, k.(2012). Polyvinyl alcohol/silver nanoparticles as a model for testing the biological activity of hybrid materials with included silver nanoparticles. *Materials Science and Engineering* **32**, 2048-2051.
14. Datta, S. C., Murti, V. V. S., Sharma, N. N., Seshadri, T. R. (1973). Glycosidic components of *Thespesia populnea* flowers. *Indian Journal of Chemistry* **11**(5), 506-7.
15. Davies, J. and Davies, D. (2010). Origins and evolution of antibiotic resistance. *Microbiol Mol Biol Rev* **74**, 417-433. PMID:20805405.
16. Dhammananda, K., Veena, G.K. and Dudhamal, T. (2016). Antimicrobial Activity of Panchavalkala powder and ointment. *International Journal of Medicinal plant and Natural Products* **2**(1), 9-15.
17. Dissanayake, M.D., Fosberg, F.R. and Clayton, W.D. (1996). *A Revised Handbook to the Flora of Ceylon*. Vol **6**, 58.
18. Doan, H.V., Riyajan, S., Iyara, R., Chudapongse, N. (2018). "Antidiabetic activity, glucose uptake stimulation and α-glucosidase inhibitory effect of *Chrysophyllum cainito* L. stem bark extract. *BMC Complementary and Alternative Medicine* **18**(1), 267.
19. El-Chaghaby, G.A. and Ahamad, A.F. (2011). Bio synthesis of silver nanoparticles using *Pistacia lentiscus* leaves extract and investigation of their antimicrobial effect. *Oriental journal of chemistry* **27**, 929-936.
20. Enit, B.D., Arumugam, V.A., Palanisamy, S.K., Puthamohan, V., Preethi, B. (2018). Phytochemistry and Pharmacology of *Ficus religiosa*. *Sys Rev Pharm* **9**(1), 45-48.

21. Ewald, A., Susanne, K., Thull, R.G., Gbureck, U. (2006). Antimicrobial titanium/silver PVD coating on titanium. *BioMed.Eng. OnLine* **5**, 22.
22. Faiyaz. A. and Asna. U. (2009). A review of Traditional uses, medicinal properties, and phytopharmacology of *Ficus racemosa*. *Pharmaceutical Biology* **48**(6), 672-681.
23. Farrukh, A. and Iqbal, A. (2003). Broad-spectrum antibacterial and antifungal properties of certain traditionally used Indian medicinal plant. *World J Microbiol Biotechnol* **19**, 653–7.
24. Ghodsieh, B., Maryam, M.T. and Mohammad, H.N. (2017). Green synthesis of silver nanoparticles using aqueous extract of saffron (*Crocus sativus* L.) wastages and its antibacterial activity against six bacteria. *Asian pacific journal of tropical biomedicine* **7**(3), 227-233.
25. Gopalakrishnan, T., Dharmaratne, M.P.J., Pieris, R.M., Wanasekara, L., Senadheera, R.K. (2017). Investigation of antibacterial activity against methicillin resistant *Staphylococcus aureus* (MRSA) and selected pharmacological properties of Panchavalkala: An Ayurvedic formulation. *International Journal of Current Research* **9**(09), 57728-57733.
26. Guerrero, L.C., Gomez-Cansino, R., Guzman-Gutierrez, S.L., et al. (2018). In vitro antiviral activity and phytochemical screen in the extracts of peels from four species of tropical fruits collected in Merida Yucatan, *Mexico. Phyton* **87**, 68–71.
27. Gunathilake, A.A.L., et al. (1984). Quaesitol, a phenol from *Garcinia quesita*. *Phytochemistry* **23**(11), 2679-2681.
28. Gurpreet, K. and Satnam, S. (2016). in-vitro antimicrobial activity of crude extract of *Ficus arnottiana* miq. leaves (moraceace): an ethnomedicinal plant. *International Journal of Pharmaceutical Sciences and Research* **7**(5), 2057-2064.
29. Hemaiswarya, S., Poonkothai, M., Raja, R., Anbazhagan, C. (2009). Comparative study on the antimicrobial activities of three Indian medicinal plants. *Egypt J Biol* **11**, 52–4.
30. He, R., Qian, X., Yin, J., Zhu, Z. (2002). Preparation of polychrome silver nanoparticles in different solvent. *J. Mat. chem* **12**, 3783-3786. doi: 10, 1039/b 205214h.
31. Hewageegana, A.U., Hewageegana, H. and Arawwawala, L.D.A.M. (2018). Comparison on phytochemical and physicochemical parameters of *Garcinia cambogia* (Gaertn.) Desr. and *Garcinia zeylanica* Linn fruit rinds. *Journal of Pharmacognosy and Phytochemistry* **7**(2), 2532-2535.
32. Hussain, A., Singh, S., Das, S.S., Anjireddy, K., Karpagam, S., Shakeel, F. (2019). Nanomedicines as drug delivery carriers of anti-tubercular drug: From pathogenesis to infection control. *Current Drug Delivery* **16**(5), 400-429.
33. Jacob, J.M., John, M.S., Jacob, A., Abitha, P., Kumar, S.S., Rajan, R., Natarajan, S., Pugazhendhi, A. (2019). Bactericidal coating of paper towels via sustainable biosynthesis of silver nanoparticles using *Ocimum sanctum* leaf extract. *Materials Research Express* **6**(4), 1.
34. Jha, A.K., Prasad, K., Prasad, K., Kulkarni, A.R. (2009). Plant system, natures nano factory. colloids and surface B. *Biointerfaces* **73**, 219-223.
35. Kalishwaralal, K., Deepak, V., Pandian, S.R.K., Kottaisamy, M., Barathmanikanth, S., Kartikeyan, B., et al. (2010). Biosynthesis of silver and gold nanoparticles using *Brevibacterium casei*. Colloids Surf B. *Biointerfaces* **77**, 257-262.
36. Kamble, M., Ashar, S., Jadhav, S. (2012). Evaluation of antibacterial activity of Panchavalkala and gel formation against multiple drug resistant strains of *S. aureus* (MRSA). *Pharma Science Monitor* **3**(1), 278.
37. Khadkutkar, D.K., (2015). A brief review of research studies conducted on Panchavalkala. *Indian Journal of Ancient Medicine and Yoga* **8**(2), 94.
38. Khalil, K.A., Fouad, H., Elsarnagawy, T., Almajhdi, F.N. (2013). Preparation and characterization of electro spun PLGA silver

composite nanofibers for biomedical applications. *Int J electrochem sei* **8**, 3483-93.
39. Kim, J.S., Kuk, E., Yu, K.N., Kim, J., Park, S.J., Lee, H.J. (2007). Antimicrobial effects of silver nanoparticles. *ElsevirInc* **3**, 95-101.
40. Kubola, J., Siriamornpun, S. and Meeso, N. (2011). Phytochemicals, vitamin C and sugar content of Thai wild fruits. *Food Chemistry* **126**(3), 972–981.
41. Kuppusamy, P., Ichwan, S.J., Parine, N.R., Yusoff, M.M., Maniam, G.P., Govinda, N. (2015). Intercellular biosynthesis of Au and Ag nanoparticles using ethanolic extract of *Brassica oleracea* L.and studies on their physiochemical and biological properties. *J. Environ. Sci* **29**, 151-157.
42. Lagbas, A., Pelisco, J.B. and Riego, V.M.P. (2016). Antibacterial activity of silver nano/microparticles in chitosan matrix prepared using *Mangifera indica* and *Chrysophyllum cainito* leaf extracts and its application in pineapple (Ananas comosus) polyester fabric. *Indian Journal of Advances in Chemical Science* **4**(1), 7–13.
43. Larue, C., Castillo-Michel, H., Sobanska, S., Cecillon, L., Burean, S., Barthes, V., et al. (2014). Foliar exposure of the croup *Lactuca sativa* to silver nanoparticles; evidence for internalization and changes in Ag speciation. *Journal of Hazardous Materials* **264**, 98 -106.
44. Liao, C., Li, Y. and Tjong, S.C. (2019). Bactericidal and cytotoxic properties of silver nanoparticles. *International Journal of molecular science* **20**(449), 1-47.
45. Liaqat, N., Jahan, N., Khalil-ur-Rahman, A.T., Qureshi, H. (2022). Green synthesized silver nanoparticles, optimization, characterization, antimicrobial activity and cytotoxicity study by hemolysis assay. *Front. chem* **10**. doi: 10.3389/f chem.2022.952006.
46. Liau, S.Y., Read, D.C., Pugh, W.J., Furr, J.R., Russell, A.D. (1997). Interaction of silver nitrate with readily identifiable group: relationship to the antibacterial action of silver ions. *Lett.Appl. Microbiol* **25**, 279-283.
47. Lusia, F. and Duncan, S. (2010). NANO YOU teachers training kit. Module **1**, 4-5.
48. Macabeo, A.G. and Lee C.A. (2014). Sterols and triterpenes from the non-polar antitubercular fraction of *Abutilon indicum*. *Pharmacognosy Journal* **6**(4), 49-52.
49. Mandal, S.C., Tapan, K., Maity, J., Das, M., Pal, S. B.P. (1999). Hepatoprotective activity of *Ficus racemosa* leaf extract on liver damage caused by carbon tetrachloride in rats. *Phytotherapy Res* **13**(5), 430–432.
50. Manimozhi, D.M., Sankar, N. and Sampath, K, G. (2012). Phytochemical screening of three medicinally important Ficus sp. *IJPRD* **4**, 44-51.
51. Matlawska, I. and Sikorska M. (2002). Flavonoid compounds in the flowers of *Abutilon indicum* (L.) Sweet (Malvaceae). *Acta Poloniae Pharmaceutica* **59**(3), 227-229.
52. Matsumura, Y., Yoshikata, K., Kunisak, S., Tsuchido, T. (2003). Mode of Bactericidal Action of Silver Zeolite and Its comparison with that of Silver Nitrate. *Appl. Environ.Microbiol* **69**, 4278-4281.
53. Mendelson, M. (2015). Role of antibiotic stewardship in extending the age of modern medicine. *S Afr Med J* **100**(5), 414-418. PMID:26242674.
54. Mittal, A.K., Chisti, Y. and Banerjee, U.C. (2013). Synthesis of metallic nanoparticles using plant extracts. *Biotecnol.Adv* **31**, 346-356.
55. Mousa, O., Vuorela, P., Kiviranta, J., Abdelwahab, S., Hiltunen, R., Vuorela, H. (1994). Bioactivity of certain Egyptian Ficus species. *J Ethnopharmacol* **41**(1-2), 71–6. PMID: 8170162.
56. Nair, R. and Chanda, S.V. (2006). Activity of some medicinal plants against certain pathogenic bacterial strains. *Indian J Pharm* **38**, 142–144.
57. Nair, R. and Chanda, S.V. (2007). Antibacterial activities of some medicinal plants of the western region of India. *Turkish J Biol* **31**, 231–236.
58. Neelakantan, S., Rajagopalan, V. and Raman, P. V. (1983). Thespesone and thespone, two new mansonone of heartwood

of *Thespesia populnea* ex Corr. (Fam. Malvaceae). *Indian Journal of Chemistry* **22B** (1), 95-6.

59. Nirasha, W.D., Chandani, K., Sanjeewani, D.M., Tharanga, P.R., Tharindra, W. (2019). screening *Garcinia zeylanica* for in-vitro antimicrobial activity and anti-oxidant activity. *Austrian journal of Technical and Natural Science* **1**, 3-10. DOI: 10.29013/AJT-20-7.8-3-10.
60. Noronha, V.T., Paula, A.J., Duran, G., Galembeck, A., Cogo-Muller, K., Franz-Montan, M., Duran, N. (2017). Silver nanoparticles in density. Dental materials **33**(10), 1110-1126.
61. Ogunlowo, O., Arimah, B. and Adebayo, M. (2013). Phytochemical analysis and comparison of in-vitro antimicrobial activities of the leaf, stem bark and root bark of *Ficus bengahalensis*. *IOSR Journal of Pharmacy* **3**, 33-38.
62. Oranusi, S.U., Braide, W. and Umeze, R.U. (2015). Antimicrobial activities and chemical compositions of *Chrysophyllum cainito* (star apple) fruit. *Microbiology Research International* **3**(3), 41–50.
63. Otari, S., Patil, R., Nadaf, N., Ghosh, S., Pawar, S. (2012). Green biosynthesis of silver nanoparticles from an actinobacteria *Rhodococcus* sp. *Mater.Lett* **72**, 92-94.
64. Park, J., Lim, D.H., Lim, H.J., Kwon, T., Choi, J.S., Jeong, S., Choi, I.-H., Cheon, J. (2011). Size dependent macrophage responses and toxicological effects of Ag nanoparticles. *Chemical Communications* **47**(15), 4383-4384.
65. Patankar, G. and Grampurohit, N.D. (1999). Detection of phytoconstituent responsible for anti-microbial activity Panchavalkala. *Aryavaidyan* **12**(4), 221-225.
66. Paulkumar, K., Gnanajobitha, G., Vanaja, M., et al. (2014). *Piper nigrum* leaf and stem assisted green synthesis of silver nanoparticles and evaluation of its antibacterial activity against agricultural plant pathogen. *The scientific journal* **9**.
67. Peter, L., Sivagnanam, S., Jayanthi, A. (2015). Synthesis of silver nanoparticles using plants extract and analysis of their antimicrobial property. Journal of Saudi chemical society **19**, 311-317.
68. Pooja, D.G. and Tannaz, J.B. (2017). Development of botanical to combat antibiotic resistance. *J Ayurveda Integr Med*, **8**(4), 266-275. PMID:28869082.
69. Prabhuji, S.K, Singh, D. K., Srivastava, A, K., Sinha, R. (2010). Antifungal activity of a new steroid isolated from *Abutilon indicum* (L.) Sw. *International Journal of Phytomedicines and Related Industries* **2**(3), 215-218.
70. Pratap, C. R., Manju, S., Vysakshi, M.V., Shaji, P.K., Achuthan, N.G. (2014). Antibacterial and Anti-fungal activities of *Thespesia populnea* leaf extracts against human pathogens. *International journal of pharma tech research* **6**(1), 290-297.
71. Priya, B., Mantosh, S., Aniruddha, M., Papita, D. (2014). Leaf extract mediated green synthesis of silver nanoparticles from widely available Indian plants: synthesis, characterization, antimicrobial property and toxicity analysis. *Bioresources and Bioprocessing* **1**(3), 1- 10.
72. Rahuman, A.A., Gopalakrishnan, G., Venkatesan, P., Geetha, K. (2008). Isolation and Identification of mosquito larvicidal compound from *Abutilon indicum* (Linn.) sweet. *Parasitology Research* **102**(5), 981-988.
73. Rajan, D.S., Rajkumar, M., Srinivasan, R., Kumarappan, C., Arunkumar, K.,Senthilkumar, K.L., Srikanth, M.V. (2013). Investigation on antimicrobial activity of root extracts of *Thespesia populnea* Linn. *Trop Biomed* **30**(4), 570-578. PMID: 24522124.
74. Rajapaksa, K.J.W., Jayasinghe, J.M.S. and Sampath, T. (2020). Determination of bioactivity and isolation of Garcinol in *Garcinia quaesita*. *Proceeding of the post graduate institute of science research congress* **133**.
75. Rajesh, S.K. and Malarkodi, C. (2014). In vitro antibacterial activity and mechanism of silver nano particles against food borne pathogens. *Bioinorganic Chemistry and Applications* **10**.

76. Rajput, A.P. and Patel, M.K. (2012). Isolation and characterization of phytoconstituents from the chloroform extract of *Abutilon indicum* leaves (Family: Malvaceae). *Asian Journal of Research in Chemistry* **5**(11), 1375-1380.
77. Rajurkar R., Jain R., Matake N., Aswar P., Khadbadi S.S., (2009). Anti-inflammatory Action of *Abutilon indicum* (L.) Sweet Leaves by HRBC Membrane Stabilization. *Research Journal of pharmacy and Technology* **2**(2), 415-416.
78. Rao Ch, V., Verma, A.R., Vijayakumar, M., Rastogi, S. (2008). Gastroprotective effect of standardized extract of *Ficus glomerata* fruit on experimental gastric ulcers in rats. *J Ethnopharmacol* **115**(2), 323–326. PMID: 17980529.
79. Rathish, N. and Sumitra, V.C. (2007). Antibacterial activities of some medicinal plants of Western region of India. *Turk. J. Biol* **31**, 231-236.
80. Reyad-Ul, F., Mehedi, R., Kawsar, M., Sharmi, S.A., Didaruzzaman. (2015). Pharmacological and Phytochemicals Potential of *Abutilon indicum*, A Comprehensive Review. *American Journal of Bioscience* **3**(2-1), 5-11.
81. Saeed, A., Huma, R., Muhammad, A., Irshad, A., Muhammad, M.H., Zafar, I., Nisar-Ur, R., (2011). Phytochemical composition and pharmacological prospectus of *Ficus bengalensis* Linn. (Moraceae)- A review. *Journal of Medicinal Plants Research* **5**(28), 6393-6400.
82. Sakhitha, K.S., Dighe, D., Santhosh, B., Parimi, S. (2013). Formulation, anti-bacterial activity and wound healing property of Panchavalkala ointment. *International Ayurvedic Medical Journal* **1**(4), 1-5.
83. Salman, H.D. (2017). Evaluation and comparison the antibacterial activity of silver nanoparticles (Ag NPs) and silver nitrate (AgNO3) on some pathogenic bacteria. *Journal of Global pharma Technology* **10**(9), 238-248.
84. Saravanan, M., Arokiyaraj, S., Lakshmi, T., Pugazhendhi, A. (2018). Synthesis of silver nanoparticles from *Phenerochaete chrysosporium* (MTCC-787) and their antibacterial activity against human pathogenic bacteria. *Microbial Pathogenesis* **117**, 68-72.
85. Sastry, M., Mayyaa, K.S. and Bandyopadhyay, K. (1997). pH Dependent changes in the optical properties of carboxylic acid derivatized silver colloid particles. Colloids and Surface A. *Physiochemical and Engineering Aspects* **127**, 221-228.
86. Sawade, H. and Tomi, H. (1997). Effect of liquid *Garcinia* extract and soluble *Garcinia* powder on body weight change, A possible material for suppressing fat accumulation. *Journal of the Japan oil chemist society* **46**(12),1467-1474.
87. Sayed, D.F., Nada, A.S., Abd El Hameed Mohamed, M., Ibrahim, M.T. (2019). Modulatory effects of *Chrysophyllum cainito* L. extract on gamma radiation induced oxidative stress in rats. *Biomedicine and Pharmacotherapy* **111**, 613–623.
88. Senarathna, U.L.N.H., Fernando, S.S.N., Gunasekara, T.D.C.P., Wanasekara, M.M., Hewageegana, H.G.S.P., et al. (2017). Enhanced antibacterial activity of TiO_2 nanoparticle surface modified with *Garcinia zeylanica* extract. *Chemistry central journal* **11**(1), 7.
89. Shaikh, W. A., Chakraborty, S., Islam, R.U. (2020). Photocatalytic degradation of rhodamine B under Uv irradiation using *Shorea robusta* leaf extract-mediated bio-synthesized silver nanoparticles. *Int J Environ Sci Technol* **17**, 2059-2072.
90. Shakeel, A., Mudasir, A., Babu, L.S., Saiqa, I. (2016). A review on plant extract mediated synthesis of silver nanoparticles for antimicrobial applications: A green expertise. *Journal of Advanced Research* **7**, 17-28.
91. Shandavi, C.B., Vikas, V.P. and Vijay, R.P. (2010). Antibacterial Activity of *Ficus bengalensis* barks on *Actinomyces viscosus*. *Int. J. Pharm. Sci* **2**(1), 39-43.

92. Shanmuganathan, R., Mubarak Ali, D., Prabakar, D., Muthukumar, H., Tajuddin, N., Kumar, S.S., Pugazhendhi, A. (2018). An enhancement of antimicrobial efficacy of biogenic and ceftriaxone-conjugated silver nanoparticles: green approach (Article). *Environmental Science and Pollution Research* **25**(11), 10362-10370.
93. Shameli, K., Bin Ahamad, M., Jaffar Al-mulla, E.A., Ibrahim, N.A., Shaban, Z. P., Rustaiyan, A., et al (2012). Green biosynthesis of silver nanoparticles using *callicarpa maingayi* stem bark extraction. *Molecules* **17**, 8506-8517. doi:10.33901 molecules 17078506.
94. Sharma, A., Sharma, R. and Singh, H. (2013). Phytochemical and Pharmacological Profile of *Abutilon Indicum* L. Sweet: A Review. *International Journal of Pharmaceutical Sciences Review and Research* **20**(1), 120-127.
95. Shastri, A. (2001). *Bhaishjya Rathnavali*. Chapter 47, verse 8 and 40. Chaukhambha Sanskrita Sanstan, Varanasi, 592-595.
96. Sheetal, A., Bagul, M.S., Prabia, M., Rajani, M. (2008). Evaluation of free radicals scavenging activity of an Ayurvedic formulation, Panchavalkala. *Indian J Pharm Sci* **70**(1), 31–8. PMID: 20390077.
97. Singh, D. and Gupta, R.S. (2008). Modulatory influence of *Abutilon indicum* leaves on hepatic antioxidant status and lipid peroxidation against alcohol-induced liver damage in rats. *Pharmacology online* **1**, 253-262.
98. Suvarna, C.H.M., Sriya, P., Arshad, M.D., Pavan. K. (2018). A review on phytochemical and pharmacological properties of *Thespesia populnea*. *Journal of Drug Delivery and Therapeutics* **8**(4), 1-4.
99. Uma, B., Prabhakar, K. and Rajendran, S. (2009). In vitro antimicrobial activity and phytochemical analysis of *Ficus religiosa* L. and *Ficus bengalensis* L. against diarrhoeal enterotoxigenic *E. coli*. *Ethnobotanical Leaflets* **13**, 472-474.
100. Valsaraj, R., Pushpangadan, P., Smitt, U.W., Adersen, A., Nyman, U. (1997). Antimicrobial screening of selected medicinal plants from India. *J Ethnopharmacol* **58**(2), 75–83. PMID: 9406894.
101. Vasudevan, M., Gunnam, K. and Parle, M. (2007). Antinociceptive and anti-inflammatory effects of *T. populnea* bark extract. *Journal of Ethnopharmacology* **109**, 264-270.
102. Veerasamy, R., Xin T.Z., Gunasagarn, S et al. (2011). Biosynthesis of silver nanoparticles using mangosteen leaf extract and evaluation of their antimicrobial activities. *J Saudi chem soc* **15**, 113-120.
103. Venkat, S.S. and Suvarna, U. (2020). A Review on Phytochemical Constituents of *Abutilon indicum* (Link) Sweet – An Important Medicinal Plant in Ayurveda. *Plantae Scientia* **3**(3), 15-19.
104. Vikas, V.P. and Vijay, R.P. (2010). *Ficus bengalensis*. An Overview. *Int. J. Pharm. Biol. Sci*. **1**(2), 1-11.
105. Wijekoon, H.P.S.K., Ekanayaka, E.M.A.K., Peiris, M.M.K., Arachchi, N.D.H., Palliyaguru, L., Kumarasinghe, U.R., Fernando, S.S.N., Jayaweera, P.M., Gunasekara, T.D.C.P. (2017). Antimicrobial activity of silver nanoparticles capped with crude extract of *Garcinia Zeylanica* and garcinol. *Proceedings of the Scientific Sessions FMS, USJ* **72**. Available at: http://dr.lib.sjp.ac.lk/handle/123456789/7634 [Accessed 28 July 2021].
106. Yazid, M.E.T., Amiri, M.S., Hosseini., H.A., *et al*. (2019). Plant -based synthesis of silver nano particles in *Handelia trichophylla* and their biological activities. *Bull Mater Sci* **42**, 155.
107. Zhang, X, F., Liu, Z.G., Shen, W., Gurunathan, S. (2016). Silver Nanoparticles: Synthesis, Characterization, Properties, Applications, and Therapeutic Approaches. *Int J Mol Sci* **17**(9), 1534. PMID: 27649147.

108. Zhang, Y., Yang, D., Kong Y., Wang, X., Pandoli, O., Gao, G. (2010). Synergetic antibacterial effect of silver nanoparticles, Aloe vera prepared via a green method. *Nano Biomed Eng* **2**(5), 970-975.

Access this Article in Online	
	Website: www.ijcrcps.com
Quick Response Code	Subject: Nanotechnology
DOI: 10.22192/ijcrcps.2025.12.09.XXX	

How to cite this article:
K.P.M.W.D.A.M.A. Fernando, J.A.M.S. Jayatilake. (2025). Green synthesis of Silver Nanoparticles with Panchavalkala and its Antimicrobial activity. Int. J. Curr. Res. Chem. Pharm. Sci. 12(9): 1-43.
DOI: http://dx.doi.org/10.22192/ijcrcps.2025.12.09.001

